



## Is the critical Shields stress for incipient sediment motion dependent on channel-bed slope?

Michael P. Lamb,<sup>1</sup> William E. Dietrich,<sup>1</sup> and Jeremy G. Venditti<sup>2</sup>

Received 14 May 2007; revised 17 October 2007; accepted 14 January 2008; published 1 May 2008.

[1] Data from laboratory flumes and natural streams show that the critical Shields stress for initial sediment motion increases with channel slope, which indicates that particles of the same size are more stable on steeper slopes. This observation is contrary to standard models that predict reduced stability with increasing slope due to the added downstream gravitational force. Processes that might explain this discrepancy are explored using a simple force-balance model, including increased drag from channel walls and bed morphology, variable friction angles, grain emergence, flow aeration, and changes to the local flow velocity and turbulent fluctuations. Surprisingly, increased drag due to changes in bed morphology does not appear to be the cause of the slope dependency because both the magnitude and trend of the critical Shields stress are similar for flume experiments and natural streams, and significant variations in bed morphology in flumes is unlikely. Instead, grain emergence and changes in local flow velocity and turbulent fluctuations seem to be responsible for the slope dependency due to the coincident increase in the ratio of bed-roughness scale to flow depth (i.e., relative roughness). A model for the local velocity within the grain-roughness layer is proposed based on a 1-D eddy viscosity with wake mixing. In addition, the magnitude of near-bed turbulent fluctuations is shown to depend on the depth-averaged flow velocity and the relative roughness. Extension of the model to mixed grain sizes indicates that the coarser fraction becomes increasingly difficult to transport on steeper slopes.

**Citation:** Lamb, M. P., W. E. Dietrich, and J. G. Venditti (2008), Is the critical Shields stress for incipient sediment motion dependent on channel-bed slope?, *J. Geophys. Res.*, 113, F02008, doi:10.1029/2007JF000831.

### 1. Introduction

[2] Predicting initial sediment motion is one of the most fundamental and practical problems in sedimentology and geomorphology. Sediment transport predictions are needed to route sediment through river networks [Cui and Parker, 2005; Cui *et al.*, 2006; Wiele *et al.*, 2007], model river incision into bedrock [Sklar and Dietrich, 2004; Lamb *et al.*, 2007], restore river functionality and habitat [Rosgen, 1996; Buffington *et al.*, 2004], and mitigate debris flows initiated from channel-beds [Papa *et al.*, 2004]. Sediment transport predictions also are crucial for understanding surface processes on planets and satellites like Mars and Titan, as they provide a straightforward and quantitatively robust method for constraining the amount of fluid that is flowing or once flowed across these planetary surfaces [Komar, 1979; Burr *et al.*, 2006; Lamb *et al.*, 2006; Perron *et al.*, 2006].

[3] Many widely used bed load sediment-transport models are based on the concept that sediment transport either

begins at, or can be scaled by, a constant value of the non-dimensional bed-shear stress or the critical Shields stress  $\tau_{*c}$  [Meyer-Peter and Müller, 1948; Engelund and Fredsoe, 1976; Luque and van Beek, 1976; Parker, 1990; Wilcock and Crowe, 2003]. The Shields stress is defined as

$$\tau_{*cg} \equiv \frac{\tau_g}{(\rho_s - \rho)gD} = \frac{u_*^2}{rgD} \quad (1)$$

where  $\tau_g$  is the shear stress at the bed, and the shear velocity  $u_* \equiv \sqrt{\tau_g/\rho}$ .  $D$  is the diameter of a particle,  $g$  is the acceleration due to gravity, and  $r$  is the submerged specific density of the sediment,  $r = (\rho_s - \rho)/\rho$ , where  $\rho_s$  and  $\rho$  are the densities of sediment and fluid, respectively. The subscript  $g$  in equation (1) is used to denote the portion of the total bed stress that is borne by sediment grains on the bed (discussed below).  $\tau_{*c}$  without further subscripts is used to describe the critical Shields criterion generically, without regard to stress partitioning.

[4] The concept of a constant Shields-stress criterion for incipient motion is based on the pioneering experimental work of Shields [1936], which showed that the Shields stress at incipient motion  $\tau_{*c}$  varies with the particle Reynolds number  $Re_p$ , but is roughly constant (i.e.,  $\tau_{*c} \approx 0.045$  [Miller *et al.*, 1977; Yalin and Karahan, 1979]) for

<sup>1</sup>Earth and Planetary Science, University of California, Berkeley, California, USA.

<sup>2</sup>Department of Geography, Simon Fraser University, Burnaby, British Columbia, Canada.

$Re_p > 10^2$  (corresponding to about  $D > 3$  mm for rivers on Earth), where

$$Re_p = \frac{u_* D}{\nu} \quad (2)$$

and  $\nu$  is the kinematic viscosity of the fluid. This result has been reproduced by many others (e.g., see review by *Buffington and Montgomery* [1997]), although significant scatter in the data exists. Theoretical models based on balancing forces on particles also have reproduced these experimental findings [e.g., *Wiberg and Smith*, 1987a; *Bridge and Bennett*, 1992].

[5] Considerable attention has been placed on sediment mixtures, in which grain shape, orientation, exposure, protrusion, and variable pocket geometry can influence the critical Shields stress [e.g., *Wiberg and Smith*, 1987a; *Kirchner et al.*, 1990; *Komar and Carling*, 1991; *Johnston et al.*, 1998]. If  $\tau_{*c}$  is a constant, then equation (1) indicates that smaller particles are more mobile, as they require less shear stress to move (Note that the term “mobility” is used herein to describe the boundary shear stress necessary to initiate sediment motion, and does not refer to the rate of bed load transport). Most studies have shown, however, that sediment is more equally mobile than that predicted by equation (1) because the differences in exposure and friction angles tend to offset differences in particle weight [*Parker et al.*, 1982; *Wiberg and Smith*, 1987a; *Parker*, 1990]. Incipient motion for mixtures then can be reasonably determined from a single function of  $\tau_{*c}$  for the bulk mixture with the representative grain diameter in equations (1) and (2) set to  $D = D_{50}$ , where  $D_{50}$  is the median grain size. Nevertheless, finer particles are generally considered to move at slightly lower shear stresses than coarser particles [e.g., *Parker*, 1990; *Ferguson*, 2003], and this difference can be more profound in steep mountain streams [e.g., *Andrews*, 1983; *Lenzi et al.*, 2006].

[6] While experimental studies on incipient particle motion have explored a wide range of parameter space, they often have been limited to moderate channel slopes and consequently the empirically determined  $\tau_{*c}$  might not be applicable to steep mountain streams or lowland rivers (Slope is defined here as  $S = \tan \beta$ , where  $\beta$  is the bed-slope angle from horizontal). Shields himself recognized a potential slope dependency of  $\tau_{*c}$  [*Shields*, 1936], but it was over 30 years before *Neill* [1967] showed that  $\tau_{*c}$  increases with increasing channel slope. *Neill* later retracted his results and stated that criticism from colleagues caused him to re-examine his data, which revealed measurement bias [*Neill*, 1968]. The original slope-dependent findings of *Neill*, however, have been reproduced subsequently for steep slopes in experimental [*Ashida and Bayazit*, 1973; *Aguirre-Pe*, 1975; *Bathurst et al.*, 1984; *Olivero*, 1984; *Graf and Suszka*, 1987; *Torri and Poesen*, 1988; *Aguirre-Pe and Fuentes*, 1991; *Picon*, 1991] and field studies [*Bartnick*, 1991; *Mueller et al.*, 2005; *Lenzi et al.*, 2006]. Detailed experiments by *Shvidchenko and Pender* [2000] and *Shvidchenko et al.* [2001] indicate that incipient motion is slope dependent even on low slopes ( $S < 0.01$ ) and for small particles ( $Re_p < 10^2$ ), which suggests that a slope-dependent Shields stress is applicable for lowland rivers as well as steep mountain streams.

[7] The reasons for an increase in critical Shields stress with increasing channel slope remain largely unexplored. Consequently  $\tau_{*c}$  is typically assumed to be independent of slope in bed load transport models (see *Shvidchenko et al.* [2001], *Papanicolaou et al.* [2004], and *Mueller and Pitlick* [2005] for notable exceptions). Theoretical models actually suggest an opposite trend to that observed; sediment should become more mobile as slope increases due to the increased component of gravity in the downstream direction [e.g., *Wiberg and Smith*, 1987a].

[8] The reduced mobility on steep slopes has been attributed to increased relative roughness of the flow (i.e.,  $k_s/h$  where  $h$  is the total flow depth and  $k_s$  is the roughness length-scale of the bed) [e.g., *Shields*, 1936; *Ashida and Bayazit*, 1973; *Buffington and Montgomery*, 1997; *Buffington and Montgomery*, 1999; *Shvidchenko and Pender*, 2000; *Mueller et al.*, 2005], since for a given total bed stress, the flow depth varies inversely with bed slope for steady uniform flow. It is true that the total flow resistance (i.e., the depth-averaged flow velocity normalized by the shear velocity, as in Manning-Strickler or Darcy-Weisbach friction relations) is a function of  $k_s/h$  for flow over hydraulically rough beds [*Nikuradse*, 1933]. It is the local near-bed velocity, however, that induces sediment motion [e.g., *Wiberg and Smith*, 1987b]. Both standard formulations for the local velocity (e.g., the log-layer profile [*Nikuradse*, 1933; *Schlichting*, 1979]) and velocity profiles corrected for particle-induced form drag [e.g., *Wiberg and Smith*, 1987b, 1991; *Nelson et al.*, 1991] predict a local near-bed flow velocity that is a function of  $z/k_s$  (where  $z$  is the height above the bed), but is independent of the total flow depth  $h$  and relative roughness  $k_s/h$ .

[9] Some have formulated models based on a critical mean flow velocity (e.g., a critical discharge [e.g., *Schoklitsch*, 1962; *Bathurst*, 1987] or a critical densimetric Froude number [e.g., *Aguirre-Pe et al.*, 2003]) for incipient motion, rather than  $\tau_{*c}$ , and claimed to find a better collapse of the data with relative roughness. As pointed out by *Gessler* [1971] and *Bettess* [1984], however, these models necessarily trend with relative roughness because the mean flow velocity is a function of the relative roughness [*Nikuradse*, 1933], and therefore are not an improvement over the Shields approach.

[10] The goal of this paper is to present a mechanistic model and a compilation of data, which indicate that the critical Shields stress for incipient motion is a function of channel slope. First we present a comprehensive collection of flume and field data for coarse particles that indicates that sediment is less mobile (larger  $\tau_{*c}$ ) on steeper slopes. Second, a simple force-balance model is formulated that allows for predictions of  $\tau_{*c}$  for single-sized sediment. Third, we hypothesize several effects that might explain the variation in  $\tau_{*c}$  with channel slope and incorporate them into the force-balance model to assess quantitatively their influence on incipient motion. The effects considered are wall drag, drag due to morphologic structures on the bed, variable friction angles, grain emergence, flow aeration, and slope-dependent variations in the structure of flow velocity and turbulent fluctuations. The results suggest that the slope dependent critical Shields stress is fundamentally due to the coincident change in  $k_s/h$  with slope for a given bed stress and roughness. Surprisingly, it is the eddy viscosity and

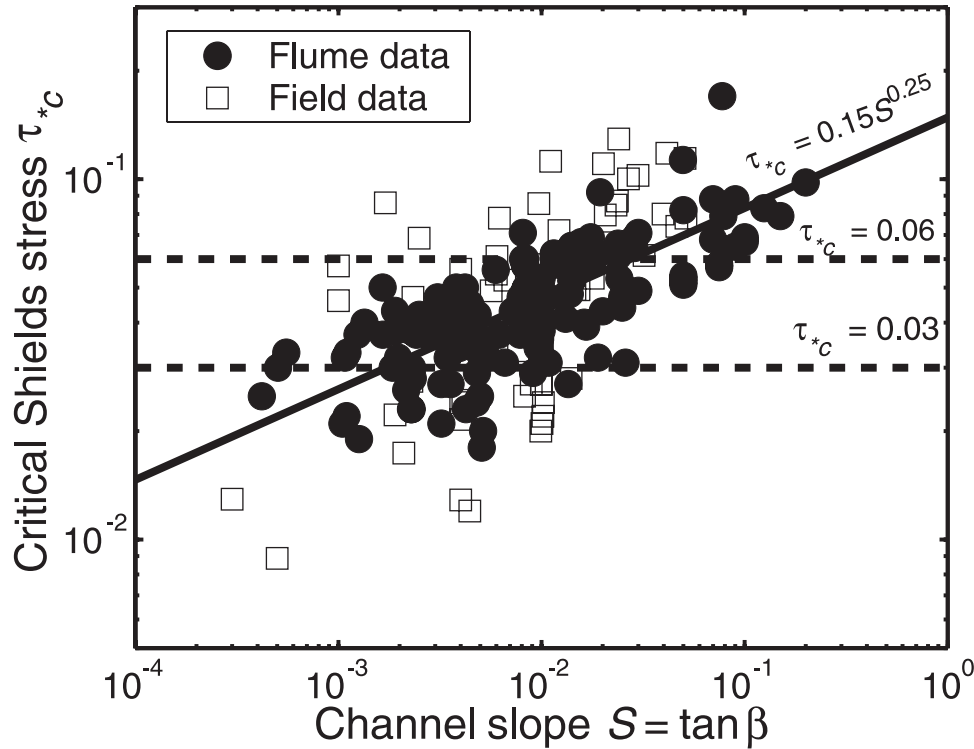


**Figure 1.** Compilation of previously published data showing the slope dependency of the critical Shields stress.  $\tau_{*c}$  is used here generically, where in actuality most of the data are based on the total stress (i.e.,  $\tau_{*cT}$ ) and some of these are corrected for wall drag (i.e.,  $\tau_{*cTR}$ ). The best fit line in a least squares sense is given by  $\tau_{*c} = 0.15S^{0.25}$  with an r-square value of 0.41. Also shown are the typical upper  $\tau_{*c} = 0.06$  and lower values  $\tau_{*c} = 0.03$  assumed for a gravel bed. The data have been filtered so that  $Re_p > 10^2$ . Data sources include *Buffington and Montgomery* [1997], *Shvidchenko and Pender* [2000], and *Mueller et al.* [2005]. Data sources previously compiled by *Buffington and Montgomery* [1997] include: *Gilbert* [1914], *Liu* [1935], *USWES* [1935], *Ho* [1939], *Meyer-Peter and Müller* [1948], *Neill* [1967], *Paintal* [1971], *Everts* [1973], *Ashida and Bayazit* [1973], *Fernandez Luque and van Beek* [1976], *Mizuyama* [1977], *Bathurst et al.* [1979, 1984, 1987], *Day* [1980], *Dhamotharan et al.* [1980], *Parker and Klingeman* [1982], *Ikeda* [1982], *Carling* [1983], *Diplas* [1987], *Graf and Suszka* [1987], *Hammond et al.* [1984], *Wilcock* [1987], *Ashworth and Ferguson* [1989], *Parker* [1990], *Komar and Carling* [1991], *Ashworth et al.* [1992], *Wilcock and McArdell* [1993], *Ferguson* [1994] and *Wathen et al.* [1995]. In addition, the data set includes the data of *Milhouis* [1973] previously compiled and analyzed by *Komar* [1987], *Wilcock and Southard* [1988], *Komar and Carling* [1991] and *Wilcock* [1993].

turbulent fluctuations that appear to depend most strongly on  $k_s/h$ , not form drag from particles or morphologic structures as is often assumed. Last, we extend the model to sediment mixtures and discuss implications for natural streams.

## 2. Data Compilation

[11] A large set of experimental and field data from incipient motion studies in unidirectional flows is presented in Figure 1. The data have been filtered so that only measurements with  $Re_p > 10^2$  are shown. By neglecting studies with  $Re_p \leq 10^2$  the flow is hydraulically rough and potential false relations with  $S$  have been avoided since, for small  $Re_p$ ,  $\tau_{*c}$  is a function of  $Re_p$  which in turn is a function of  $S$  (see *Buffington and Montgomery* [1997] for discussion). Thus the data in Figure 1 represent the regime

where  $\tau_{*c}$  is thought to be a constant ranging from 0.03 to 0.06 [*Buffington and Montgomery*, 1997]. *Yalin and Karahan* [1979] and *Wilcock* [1993], for example, suggested a constant  $\tau_{*c}$  value of 0.047 for mixed size gravel, which is widely used. It is clear from Figure 1 that much of the data does not fall within  $0.03 < \tau_{*c} < 0.06$ . Moreover, despite data scatter, there is a trend of increasing critical Shields stress with channel slope. A best fit line to all data (in a least squares sense) is shown in Figure 1 and is given by

$$\tau_{*c} = 0.15S^{0.25} \quad (3)$$

[12] The data are separated according to the environment where they were collected: laboratory flumes or natural streams (field). Both data sets appear to have a similar magnitude and trend of  $\tau_{*c}$  with channel slope. There is an obvious lack of data for  $S < 10^{-3}$  and  $S > 10^{-1}$ , the former

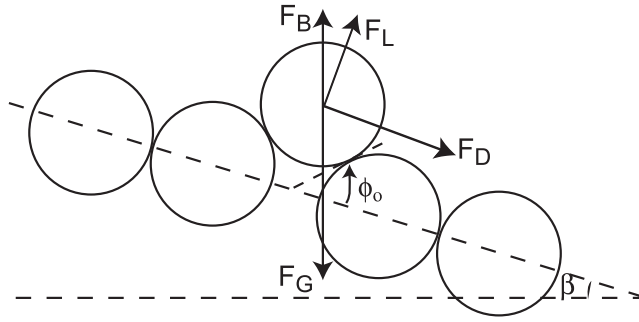


**Figure 2.** Force balance on a grain (modified from *Wiberg and Smith* [1987a]).  $F_B$ ,  $F_L$ ,  $F_D$  and  $F_G$  are the forces due to buoyancy, lift, drag and gravity, respectively.  $\phi_0$  is the friction angle and  $\beta$  is the bed-slope angle.

is likely due to the bed being sand covered in natural rivers (i.e.,  $Re_p \leq 10^2$ ).

[13] The scatter in the data probably is due to differences in friction angles, drag from channel walls and morphologic structures on the bed, sediment shapes, and size distributions. In addition, there is variability in the criteria for defining incipient motion [*Buffington and Montgomery*, 1997]. This notwithstanding, the trend of increasing  $\tau_{*c}$  with  $S$  is significant despite the fact that the data have not been corrected to account for these effects. The remainder of the paper is devoted to explaining the overall trend in the data by balancing forces about a particle.

### 3. Force Balance Model

[14] In stream flow, the buoyancy force  $F_B$ , lift force  $F_L$ , and drag force  $F_D$  act to mobilize particles, while the force due to gravity  $F_G$  holds particles in place (Figure 2) [e.g., *Wiberg and Smith*, 1987a]. Initial particle motion occurs when these forces are balanced (in the coordinate system parallel to the streambed), i.e.,

$$F_D + (F_G - F_B) \sin \beta = [(F_G - F_B) \cos \beta - F_L] \tan \phi_0 \quad (4)$$

where  $\phi_0$  is the friction angle between grains and  $\beta$  is the bed-slope angle ( $S \equiv \tan \beta$ ). In this model, we neglect the possibility that particles might move due to undermining. In equation (4),  $F_B$  is taken to be in the vertical direction, rather than perpendicular to the water surface as is sometimes assumed [*Mizuyama*, 1977; *Christensen*, 1995], based on the discussion of *Chiew and Parker* [1995]. We define the forces acting on a particle as follows:

$$F_D = \frac{1}{2} C_D \rho \langle u^2 \rangle A_{xs} \quad (5)$$

$$F_L = \frac{1}{2} C_L \rho \langle u^2 \rangle A_{xs} \quad (6)$$

$$F_B = \rho g V_{ps} \quad (7)$$

$$F_G = \rho_s g V_p \quad (8)$$

where  $C_D$  and  $C_L$  are the drag and lift coefficients, respectively.  $V_p$  is the total volume of the particle. In this derivation, we allow for the fact that a portion of the particle might be emergent from the flow at incipient motion. Thus  $A_{xs}$  is the cross-sectional area of the particle that is perpendicular to and exposed to the flow.  $A_{xs}$  does not include any portion of the particle that is emergent from the flow or within the zero-velocity region near the bed [*Kirchner et al.*, 1990]. Likewise,  $V_{ps}$  is the submerged volume of the particle and equals  $V_p$  only if the particle is fully submerged.  $\langle u^2 \rangle$  is local velocity squared and spatially averaged over  $A_{xs}$ . Equations (5)–(8) can be combined and rearranged in terms of a critical Shields stress as,

$$\tau_{*cg} = \frac{u_*^2}{rgD} = \frac{2}{C_D} \frac{u_*^2}{\langle u^2 \rangle} \cos \beta \left( \frac{\tan \phi_0 - \tan \beta}{1 + (F_L/F_D) \tan \phi_0} \right) \cdot \left[ \frac{V_p}{A_{xs} D} \frac{1}{r} \left( \frac{\rho_s}{\rho} - \frac{V_{ps}}{V_p} \right) \right]. \quad (9)$$

Equation (9) is identical to the formula derived by *Wiberg and Smith* [1987a] except for the term in the brackets, which accounts for grain emergence and is equal to a constant (i.e., a grain-shape factor) for a fully submerged particle.

[15] Equation (9) has been written in terms of the portion of shear stress that acts on the sediment grains  $\tau_g$ . In practice, the Shields stress more often is calculated from laboratory or field measurements of the total driving stress at the bed  $\tau_T$ , which is a sum of the stress spent on the channel walls  $\tau_w$ , bed morphology  $\tau_m$ , and the particles of interest on the bed  $\tau_g$  [e.g., *Einstein and Barbarossa*, 1952; *Vanoni and Brooks*, 1957; *Smith and McLean*, 1977], i.e.

$$\tau_T = \tau_g + \tau_m + \tau_w. \quad (10)$$

Note that we use the term *morphologic drag* (i.e.,  $\tau_m$ ) to describe the portion of the total stress spent on collections of particles and other bed morphologic structures that are larger than the individual grain scale. *Morphologic drag* is used instead of the more common term *form drag* because each individual component of stress in equation (10) (i.e.,  $\tau_g$ ,  $\tau_m$  and  $\tau_w$ ) can result from a combination of viscous skin-friction stresses and form-drag stresses [e.g., *McLean and Nikora*, 2006], although form drag dominates for high roughness Reynolds numbers. For steady and uniform flow conditions, the total stress at the bed can be calculated from

$$\tau_T = \rho g h \sin \beta. \quad (11)$$

In practice, the low-slope approximation of  $\sin \beta \approx \tan \beta \equiv S$  is often employed. By combining equations (1) and (9)–(11), we formulate a version of the critical Shields stress  $\tau_{*cT}$  that incorporates both the total stress and the low-slope approximation as

$$\tau_{*cT} = \frac{hS}{rD} = \frac{2}{C_D} \frac{u_*^2}{\langle u^2 \rangle} \left( \frac{\tau_T}{\tau_T - \tau_m - \tau_w} \right) \left( \frac{\tan \phi_0 - \tan \beta}{1 + (F_L/F_D) \tan \phi_0} \right) \cdot \left[ \frac{V_p}{A_{xs} D} \frac{1}{r} \left( \frac{\rho_s}{\rho} - \frac{V_{ps}}{V_p} \right) \right] \quad (12)$$

As can be seen by inspection of equation (12), the term  $\tan \beta$  will cause  $\tau_{*cT}$  to decrease with increasing channel slope, which is counter to the observations (Figure 1). This indicates that, for a given particle size  $D$ , at least one of the other variables in equation (12) must depend on channel slope or flow depth  $h$  in such a way that produces increasing  $\tau_{*cT}$  with increasing channel slope. Below, several of the terms in equation (12) are considered.

#### 4. Potential Slope Dependent Effects

[16] In this section wall drag, drag from morphologic structures on the bed, variable friction angles, grain emergence, air entrainment, variable drag and lift coefficients, the local vertical-velocity profile, and the structure of turbulent velocity fluctuations are considered as potential causes for the slope dependency of  $\tau_{*cT}$ . In section 5, these effects are quantified and incorporated into the force balance (equation (12)) to assess their importance on incipient motion.

##### 4.1. Wall Drag

[17] Wall drag ( $\tau_w$ ) is the portion of the driving stress that is spent on the channel banks. In rectangular channels where the channel bed and walls are equally rough, the wall drag can be calculated from  $\tau_w = (2h/w)\tau_g$  [Vanoni and Brooks, 1957]. Thus wall drag becomes important for channels with small width-to-depth ratios. For this case, a critical Shields number that incorporates wall drag  $\tau_{*cTR}$  can be written by substituting  $\tau_w = (2h/w)\tau_g$  and equation (10) into equation (12) and rearranging, as

$$\tau_{*cTR} = \frac{RS}{rD} = \frac{2}{C_D} \frac{u_*^2}{\langle u^2 \rangle} \left( \frac{\tau_T}{\tau_T - \tau_m} \right) \left( \frac{\tan \phi_0 - \tan \beta}{1 + (F_L/F_D) \tan \phi_0} \right) \cdot \left[ \frac{V_p}{A_{xs} D r} \left( \frac{\rho_s}{\rho} - \frac{V_{ps}}{V_p} \right) \right] \quad (13)$$

where the hydraulic radius is  $R = wh/(w + 2h)$ . Note that this formulation for the wall drag should not be used when the wall roughness is substantially different than that on the bed. For example, in flume experiments with smooth walls,  $\tau_w$  will be much smaller [Johnson, 1942; Houjou et al., 1990].

[18] Neglecting wall corrections could result in a slope-dependent critical Shields stress if the width-to-depth ratios of flows at incipient motion decrease, or the roughness of the channel walls relative to the bed increase with channel slope. The former is likely true in natural channels where the bankfull width-to-depth ratio tends to be inversely related to channel slope [e.g., Parker et al., 2007]. This notwithstanding, a partial or full wall correction (see Buffington and Montgomery [1997] for discussion) has been applied to the much of the data presented in Figure 1 [e.g., Gilbert, 1914; Liu, 1935; U.S. Waterways Experimentation Station (USWES), 1935; Meyer-Peter and Müller, 1948; Neill, 1967; Paintal, 1971; Everts, 1973; Ashida and Bayazit, 1973; Fernandez Luque and van Beek, 1976; Ikeda, 1982; Mizuyama, 1977; Bathurst et al., 1987; Graf and Suszka, 1987; Wilcock, 1987, 1993; Ashworth and Ferguson, 1989; Ashworth et al., 1992; Wilcock and McArdell, 1993; Shvidchenko and Pender, 2000]. Moreover, many of these

individual studies show a slope-dependent critical Shields stress [e.g., Ashida and Bayazit, 1973; Mizuyama, 1977; Bathurst et al., 1987; Graf and Suszka, 1987; Shvidchenko and Pender, 2000]. Therefore other factors besides wall drag must be responsible for the slope-dependent critical Shields stress.

##### 4.2. Bed Morphology and Friction Angles

[19] Changes to the bed morphology with channel slope might affect the incipient motion criteria given by equation (12) through variations in the stress borne on morphologic structures ( $\tau_m$ ), friction angles ( $\phi_0$ ), or both. It is common to assume that the trend of increasing critical Shields stress with slope is due to an increase in drag caused by morphologic structures on the bed ( $\tau_m$ ) [Buffington and Montgomery, 1997; Mueller et al., 2005; Lenzi et al., 2006; Parker et al., 2007]. The stress spent on morphologic structures usually is dominated by form drag due to flow separation, wakes, and secondary currents caused by particle clusters [Brayshaw et al., 1983; Hassan and Reid, 1990], stone cells [Church et al., 1998; Hassan and Church, 2000], bars [Parker and Peterson, 1980; Millar, 1999], woody debris [Braudrick and Grant, 2000; Manga and Kirchner, 2000], immobile or protruding particles [Wiberg and Smith, 1991; Nelson et al., 1991; Millar, 1999; Yager et al., 2007] or step-pools [Bathurst, 1985; Aberle and Smart, 2003; Wilcox et al., 2006].

[20] The magnitude of form drag due to flow separation in turbulent flow is proportional to the size and concentration of the roughness elements, and the square of the local flow velocity about the elements [e.g., Batchelor, 1967; Smith and McLean, 1977]. Thus the hypothesized increase in morphologic drag on steeper slopes could be due to changes in the bed morphology that increase roughness. For example, if the size or concentration of morphologic structures on the channel bed increase with increasing channel slope, then this could cause greater morphologic drag ( $\tau_m$ ) and larger  $\tau_{*cT}$  on steeper slopes (equation (12)). These effects are undoubtedly important in natural streams [Millar, 1999; Buffington et al., 2004], but are not important in flume experiments where the same sediment of near-uniform size was used on different slopes, and the sediment beds were leveled before each experiment.

[21] In addition to morphologic drag, systematic changes in the friction angle  $\phi_0$  with increasing channel slope also might be responsible for the trend in  $\tau_{*c}$  with slope. Variations in friction angles can occur in natural streams because of differences in shapes, orientations, and sorting of the supplied sediment [Kirchner et al., 1990; Buffington et al., 1992; Johnston et al., 1998; Armanini and Gregoretti, 2005]. The morphologic structures described above could cause larger  $\phi_0$  if grains form more stable patterns [Brayshaw et al., 1983; Hassan and Church, 2000; Church and Hassan, 2002]. In addition, bimodal size distributions (e.g., sand and gravel) can have a smoothing effect by reducing friction angles and consequently  $\tau_{*cT}$  [Wilcock, 1998; Wilcock and Crowe, 2003], and sand might be more prevalent in lower sloping rivers. Nonetheless, like morphologic drag, a systematic increase in friction angles with channel slope is an unlikely result for flume experiments where the sediment mixture was held constant at different channel slopes.

[22] Since variations in morphologic structures and friction angles with channel slope are deemed unimportant in flume experiments, a comparison between flume and field data allows for the assessment of these effects in natural streams. Surprisingly, there is no distinct difference in either the magnitude of  $\tau_{*c}$  or the trend with channel slope between field and flume data (Figure 1). It is possible that there is some effect of increasing morphologic drag or friction angles for  $S > 0.02$  as much of the field data plot above the regression line for these slopes. The field data, however, are also more scattered than the flume data, which could be due to more variable morphologic drag in the field (or other effects discussed above). Nonetheless, like the flume data, it seems reasonable to conclude that morphologic drag and variable friction angles are not primarily responsible for the observed slope dependency in the field.

### 4.3. Grain Emergence

[23] One obvious effect that would cause reduced mobility with increasing slope is grain emergence [Graf, 1979]. As a particle emerges from the flow, both the area of the particle that is exposed to the flow  $A_{xs}$  and the buoyancy force on the particle are reduced, which results in reduced mobility with increasing slope. This can be seen in the term  $\left[ \frac{V_p}{A_{xs} D} \frac{1}{r} \left( \frac{\rho_s}{\rho} - \frac{V_{ps}}{V_p} \right) \right]$  in equation (12), which becomes large with particle emergence. This, however, cannot fully explain the observed trend because a slope-dependent Shields criterion has been documented for  $S < 10^{-2}$  when grains were well submerged (Figure 1) [Shvidchenko and Pender, 2000]. At incipient motion, particles typically are not emergent from the flow for  $S < \sim 10^{-1}$  [Ashida and Bayazit, 1973].

### 4.4. Air Entrainment

[24] To our knowledge, Wittler and Abt [1995] were the first to suggest that aeration would result in reduced mobility with increasing channel slope due to a reduction in the density of the water-air mixture. Aeration also can affect the mean flow velocity and the corresponding bulk friction factor [Straub et al., 1954; Straub and Lamb, 1956; Chanson, 2004]. The mean flow velocity increases with increased aeration because of reduced drag, so it is probable that these two effects offset one another when assessing the drag force on a particle. Because of the lack of data, only reduced fluid density with aeration is considered here.

[25] From continuity, the density of the air-water mixture  $\rho$  can be written as

$$\rho = \rho_w(1 - c_a) \quad (14)$$

where  $\rho_w$  is the density of water,  $c_a$  is the volumetric concentration of air, and the mass of air is assumed negligible. The equilibrium concentration of air in open-channel flow has been shown to be a strong function of channel slope. Chanson [1994] fit the relationship

$$c_a = 0.9 \sin \beta \quad (15)$$

to experimental data [Straub and Anderson, 1958; Aivazyan, 1987] and suggested that the relationship is independent of flow discharge, velocity, and channel roughness. None-

theless, equation (15) probably underestimates the air concentration in natural streams because it does not take into account large roughness elements that can enhance mixing. For example, air concentrations of 0.1 to 0.4 have been measured in the wake of a hydraulic jump in a natural stream with a reach-averaged bed slope of about 0.04 [Valle and Pasternack, 2006]. Equation (15) only predicts an air concentration of 0.036 for the same slope.

[26] Stream aeration appears to be a plausible mechanism for an increase in  $\tau_{*c}$  with increasing channel slope. Equations (14) and (15) indicate that the fluid density would decrease with increasing channel slope due to aeration. A reduction in fluid density decreases the drag on the particles and the buoyancy force, which both increase particle stability (equation (12)). As will be shown in section 5, however, aeration cannot fully explain the observed slope dependence of the critical Shields criterion because significant aeration only occurs for steep slopes.

### 4.5. Drag and Lift Coefficients

[27] The drag coefficient  $C_D$  is typically thought to be independent of channel slope, with a constant value of about 0.4 to 0.5 for large particle Reynolds numbers based on the settling velocity of spheres [Schlichting, 1979]. Direct measurements using a force transducer suggest that this is an underestimate and that  $C_D \cong 0.9$  [Nelson et al., 2001; Schmeckle et al., 2007]. Very few studies have measured  $C_D$  under shallow flows or on steep slopes. One notable exception is the study of Flammer et al. [1970], which showed that drag can increase by an order of magnitude for shallow flows due to back-water effects and an associated pressure differential across a particle referred to as *wave-drag*. Later experiments have confirmed this trend [Lawrence, 2000; Carling et al., 2002]. Unfortunately, these relationships are difficult to incorporate into a force balance because  $C_D$  was measured as a function of the depth-averaged velocity rather than the local velocity around the grain. Because the depth-averaged velocity is a function of the relative roughness  $k_s/h$  and the local velocity about the grains is not (as discussed in section 1), these measurements might falsely indicate increasing  $C_D$  with increasing relative roughness. Caution also should be used when applying these results to natural settings because the measurements were often made on isolated particles in an otherwise flat flume bed. Particles, when isolated, provide a more significant obstacle to the flow than for a packed sediment bed, and therefore might produce a larger pressure differential. If the wave-drag hypothesis is correct, incorporating the additional pressure differential would produce decreasing  $\tau_{*c}$  with increasing slope, which is opposite of the observed trend (Figure 1). Therefore this cannot be the mechanism for increasing  $\tau_{*c}$  with channel slope.

[28] Several studies have pointed to the fact that  $C_D$  might have a particle Reynolds number dependence even for large  $Re_p$  where  $\tau_{*c}$  is thought to be Reynolds-number independent. For isolated spheres with  $Re_p > 10^5$ ,  $C_D$  is known to decrease from 0.5 to about 0.2, which is deemed the *drag crisis* [Schlichting, 1979; Shen and Wang, 1985]. Shvidchenko and Pender [2000] showed that  $\tau_{*c}$  decreased with increasing  $Re_p$  (for constant  $S$ ) even for  $10^2 < Re_p < 10^5$ . Figure 3 shows the incipient motion data stratified according to  $Re_p$ . There might be a slight trend of increasing

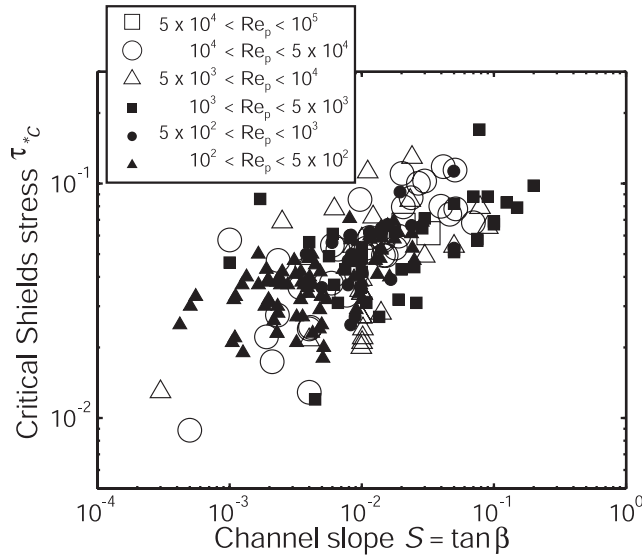


**Figure 3.** Incipient motion data from Figure 1 stratified according to particle Reynolds number  $Re_p$ .

$\tau_{*c}$  with increasing  $Re_p$ , but this is due to the dependence of  $Re_p$  on  $S$  and should not be considered important. Looking at the variation in  $\tau_{*c}$  along lines of equal slope, there does not appear to be a significant Reynolds number dependence. There are no data for  $Re_p > 10^5$ , such that the effect of the drag crises cannot be determined.

[29] Little work has been done on measuring the lift coefficient, especially in steep streams with low particle submergence. Recent direct measurements indicate that lift does not scale with the velocity difference across a grain [Nelson et al., 2001; Schmeckle et al., 2007], which is inconsistent with expectations of flow according to the Bernoulli principle. It seems possible that lift forces might become less important when grains emerge from the flow, although pressure fluctuations within a porous bed can still cause lift on emergent particles [Smart, 2005; Vollmer and Kleinhans, 2007]. The lack of data and theory make it difficult to incorporate lift into a force balance at present [Nelson et al., 2001; Schmeckle and Nelson, 2003; Schmeckle et al., 2007].

#### 4.6. Structure of Average Flow Velocity

[30] The remaining process that could be responsible for the decrease in mobility with increasing slope is the structure of the local flow velocity, i.e.,  $u/u_*$  in equation (12). The double-averaged component of the flow velocity  $\bar{u}$  (i.e., averaged in time and space [e.g., McLean and Nikora, 2006]) is considered here and turbulent fluctuations are discussed in section 4.7. The flow velocity  $\bar{u}$  is typically described as varying logarithmically near the bed [Schlichting, 1979],

$$\frac{\bar{u}(z)}{u_*} = \frac{1}{\kappa} \ln\left(\frac{z}{z_0}\right) \quad (16)$$

where  $z$  is the height above the bed,  $\kappa$  is von Karman's constant of 0.41, and  $z_0 = k_s/30$  for hydraulically rough flow [Nikuradse, 1933]. There is no total depth ( $h$ ) dependency

in equation (16), hence the local velocity is predicted to be independent of relative roughness  $k_s/h$  and channel slope for a given shear stress (Figure 4). For example, given a constant roughness height  $k_s$  and total shear stress, an increase in the flow depth is predicted to have no effect on the velocity at any location above the bed. This is the basis for the conclusion by many [e.g., Yalin, 1977] that incipient motion does not depend on the relative roughness.

[31] Equation (16), however, is a poor predictor of the velocity around particles. Within the so-called *roughness layer*, the flow around sediment particles is strongly 3-D and influenced by wakes shed by grains [Nowell and Church, 1979; Schmeckle and Nelson, 2003]. A unified theory does not yet exist for velocity profiles in the roughness layer, but observations in mountain streams have shown that the velocity profile can deviate strongly from logarithmic [e.g., Byrd and Furbish, 2000; Wohl and Thompson, 2000].

[32] Some authors have suggested that, for the same bed shear stress, an increase in relative roughness causes a decrease in flow velocity around bed particles [e.g., Ashida and Bayazit, 1973; Bayazit, 1978; Graf, 1991; Shvidchenko and Pender, 2000; Vollmer and Kleinhans, 2007]. This hypothesis is partially supported by the experiments of Chiew and Parker [1994]. They measured the conditions of incipient motion on variable slopes in a sealed duct and were thus able to vary slope while holding the relative roughness constant. Contrary to the open-channel experiments in Figure 1, Chiew and Parker [1994] showed that  $\tau_{*c}$  decreased with increasing channel slope due to the increased gravitational component in the downstream direction. These experiments, therefore, indicate that the observed increase in  $\tau_{*c}$  with increasing slope in open-channel flow is fundamentally due to the coincident increase in relative roughness (for the same boundary shear stress and particle size), although lack of aeration also might have been a factor.

[33] There are several 1-D models for flow velocity within roughness elements, drawing largely on atmospheric boundary layer studies [e.g., Raupach et al., 1991] or flow through vegetation [e.g., Lightbody and Nepf, 2006]. Katul et al. [2002] suggested a hyperbolic tangent function, but their relationship is only valid for  $h > D$  because the inflection point at  $z = D$  must be specified. Nikora et al. [2001, 2004] and McLean and Nikora [2006] have suggested constant, linear, and exponential velocity profiles within the roughness layer, based on different scaling arguments utilizing the double-averaged equations of motion. All of these models, however, predict a local velocity that is independent of relative roughness, which is contrary to available data [Bayazit, 1975; Tsujimoto, 1991]. Thus applying these models to incipient particle motion would not result in the observed slope-dependent critical-Shields stress.

[34] Relative roughness might affect velocity profiles by (1) reducing the stress borne by the fluid due to particle-induced form drag or (2) by changing the deformability of the fluid (i.e., its eddy viscosity) for a given bed stress. For example, the models of Wiberg and Smith [1987b, 1991] and Nelson et al. [1991] considered both of these effects. These models showed that particle-induced form drag does affect local velocity profiles, and for a given total stress, form drag is a function of the bed roughness-length scale  $k_s$ ,

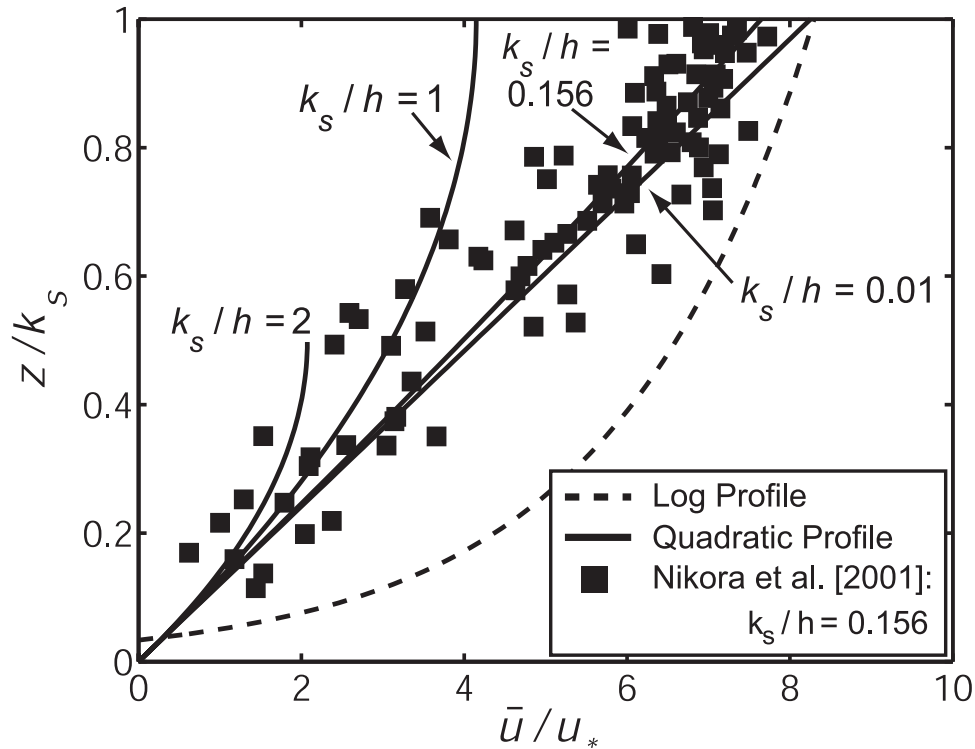


**Figure 4.** Velocity predictions for a logarithmic profile (equation (16)) and the quadratic profile (equation (20)) for different cases of relative roughness  $k_s/h$ . The height above the bed  $z$  is non-dimensionalized by the bed-roughness length scale  $k_s$ . The stream-wise velocity  $\bar{u}$  is non-dimensionalized by the shear velocity  $u_*$ . The black squares are experimental measurements, which we have digitized from Figure 4b of *Nikora et al.* [2001]. In their original figure many data points overlap where  $z/k_s > 0.5$ , such that we have under sampled their data in this region. Note that the log profile is independent of  $k_s/h$ .

as well as the concentration of roughness elements. Nonetheless, the models also suggest that for a given  $k_s$ , particle-induced form drag is not a function of flow depth, relative roughness or channel slope. We emphasize here that flow resistance is not equivalent to particle form drag. Flow resistance is a non-dimensional quantity that relates the depth-averaged flow velocity to the shear velocity, as in the Manning-Strickler and Darcy-Weisbach flow-resistance relations, and it necessarily is a function of  $(k_s/h)$  because the flow velocity is integrated over the total depth. Particle form drag, on the other hand, is a force due to pressure differentials about particles from wakes, and it scales with the local velocity around the particles [Batchelor, 1967], not the depth-averaged velocity. For simplicity, and because particle form drag appears to be independent of slope and  $k_s/h$  (for the same total shear stress), a particle-form-drag correction for the local flow velocity [e.g., *Wiberg and Smith*, 1991] is not attempted here.

[35] The second way that relative roughness might affect the local flow velocity is through changes in fluid deformation (i.e., eddy viscosity) induced by mixing from wakes shed by particles. To explore this effect, we formulate a simple and plausible expression for the flow velocity within the roughness layer based on a mixing-length that is a function of bed roughness. The vertical structure of flow velocity in steady and uniform open-channel flow can be

derived from an eddy viscosity approach [Schlichting, 1979] as

$$\tau(z) = \rho u_*^2 \left(1 - \frac{z}{h}\right) = \rho L^2 \left(\frac{d\bar{u}}{dz}\right)^2 = \rho u_* L \frac{d\bar{u}}{dz} \quad (17)$$

where  $L$  is the mixing length. This statement for the fluid shear stress uses the Boussinesq hypothesis that  $\tau(z) = \rho \varepsilon d\bar{u}/dz$  and assumes that the eddy viscosity ( $\varepsilon$ ) can be approximated from the product of local turbulent velocity and length scales (i.e.,  $u_* L$ ). The parameterization of the total stress as  $\tau(z) = \rho u_*^2 (1 - z/h)$  is valid for an impermeable bed, but is an approximation near a sediment bed [McLean and Nikora, 2006].

[36] Typically, the mixing length is set to

$$L = \kappa z \left(1 - \frac{z}{h}\right), \quad (18)$$

which, when combined with equation (17), yields the well-known logarithmic velocity profile given by equation (16). Inspection of equations (17) and (18) reveals that the depth dependencies (i.e., the term  $(1-z/h)$ ) cancel when these equations are combined resulting in a self-similar velocity profile (equation (16)) that is independent of relative roughness (Figure 4).

[37] In the near-bed region, mixing instead should be dominated by wakes shed by the particles [Lopez and Garcia, 1996; Nikora et al., 2001; Defina and Bixio, 2005]. Within the roughness layer it is appropriate to define the mixing length as

$$L = \alpha_1 k_s, \quad (19)$$

where  $\alpha_1$  is a constant of proportionality that is likely less than unity [Schlichting, 1979; Wiberg and Smith, 1987b, 1991; Nelson et al., 1991]. Combining equation (17) and (19) and integrating, results in a quadratic velocity profile,

$$\frac{\bar{u}}{u_*} = \frac{z}{\alpha_1 k_s} \left( 1 - \left( \frac{z}{2k_s} \frac{k_s}{h} \right) \right) \quad (20)$$

where the no-slip boundary condition  $\bar{u}(z=0) = 0$  has been applied. Note that applying a no slip condition at  $z_0$  rather than  $z = 0$  does not yield a significant difference in our model predictions. The coefficient was found to be  $\alpha_1 = 0.12$  by matching equations (16) and (20) at  $z = k_s$  and assuming deep flow ( $h \gg k_s$ ). This value is similar to those proposed previously for equation (19) (e.g., 0.18: Schlichting [1979] and Nelson et al. [1991]; 0.41: Wiberg and Smith [1991]).

[38] Equation (20) should hold only in the roughness layer and above this region a more appropriate velocity profile would be logarithmic. In addition, equation (20) might be invalid for  $h < k_s$ , because the dominant mixing length is likely smaller than  $k_s$  if particles are emergent from the flow. To our knowledge, no studies have measured the mixing length or the velocity profile in emergent gravel. For simplicity, we assume that equation (20) is valid within the roughness layer ( $z < k_s$ ) for all values of relative roughness ( $k_s/h$ ).

[39] By using a constant mixing length (i.e., one that does not vary linearly with  $(1-z/h)$ ), the local velocity about the grains (equation (20)) is now predicted to depend on relative roughness  $k_s/h$ . For deep flow (small relative roughness), the quadratic profile is near linear within the roughness layer and matches the logarithmic profile at  $z = k_s$  (Figure 4). This linear profile is consistent with the measurements of Dittrich and Koll [1997] and Nikora et al. [2001], the later of which are shown for the case  $k_s/h = 0.156$  (Figure 4). The data do not support the logarithmic profile. For shallow flow, the quadratic profile predicts slower flow velocity than the logarithmic profile, especially near the top of the roughness layer. The logarithmic profile, on the other hand, is self-similar for all values of relative roughness, such that they plot on the same curve (Figure 4). Unfortunately, owing to the difficulty of measurements within the roughness layer, we know of no other data to test the model. The model is consistent, however, with the measurements of Bayazit [1975] that showed that flow velocity near the top of the roughness elements systematically decreases with increasing relative roughness.

[40] Note that the change in local velocity as a function of relative roughness predicted by equation (20) will necessarily produce a change in particle form drag, since form drag depends on the local velocity [e.g., Wiberg and Smith, 1991]. Nonetheless, this is an indirect effect and the

dependency of local-flow velocity on relative roughness appears to be due to changes in the eddy viscosity for a given bed stress, and not due to a reduction in stress due to increased form drag.

#### 4.7. Turbulent Fluctuations

[41] Many studies have shown that the local average velocity  $\bar{u}$  is not the only relevant velocity scale in determining sediment mobility and, in addition, the fluctuations due to turbulence should be considered [e.g., Grass, 1970; Jackson, 1976; Bayazit, 1978; Best, 1992; Chang, 1998; Sechet and Le Guennec, 1999; Papanicolaou et al., 2002; Schmeeckle and Nelson, 2003; Zanke, 2003; Wu and Yang, 2004; Hofland et al., 2005; Cheng, 2006; Vollmer and Kleinhans, 2007], particularly in steep streams where the velocity profile is not logarithmic [Furbish, 1993, 1998; Furbish et al., 1998; Byrd and Furbish, 2000]. Of importance for bed load transport are outward interactions generated from wakes shed by roughness elements [Nelson et al., 1995; Papanicolaou et al., 2001] and downward-directed intrusions of high momentum fluid that contribute to the Reynolds stress (i.e., sweeps) [Sutherland, 1967; Nakagawa et al., 1980; Drake et al., 1988; Best, 1992]. The frequency of sweep events scale with the depth-averaged flow velocity and flow depth [Rao et al., 1971; Nezu and Nakagawa, 1993; Shvidchenko and Pender, 2001; Marquis and Roy, 2006] (i.e., outer scaling), rather than the inner parameters of kinematic viscosity and shear velocity. In addition to turbulent fluctuations within the flow, pressure fluctuations within the pore fluid of the bed are important in inducing sediment motion [Smart, 2005; Vollmer and Kleinhans, 2007].

[42] The intensity of turbulent fluctuations (i.e.,  $\sigma_u/u_*$  where  $\sigma_u$  is the root-mean square of stream-wise velocity) varies with height above the bed and has a peak value near the bed in hydraulically smooth flow, or near the top of the roughness elements in hydraulically rough flow [Raupach et al., 1991; Nikora and Goring, 2000]. This peak value (i.e.,  $\sigma_{u,\max}/u_*$ ) has been called a “universal constant” [Nezu and Nakagawa, 1993] and typical values range from 2.2 to 2.8. Most studies, however, have focused on small relative roughness, i.e.,  $h \gg k_s$  [Kironoto and Graf, 1994; Song et al., 1994; Wang and Dong, 1996; Nikora and Goring, 2000; Tachie et al., 2000, 2004; Wu and Yang, 2004] or hydraulically smooth beds [e.g., Nezu and Rodi, 1986]. We are aware of only four studies that have measured  $\sigma_{u,\max}/u_*$  for a wide range of relative roughness [Bayazit, 1975; Wang et al., 1993; Dittrich and Koll, 1997; Carollo et al., 2005]. These studies show that  $\sigma_{u,\max}/u_*$  is not a universal constant, but instead increases as depth increases relative to the roughness-length scale of the bed.

[43] Figure 5 shows a compilation of  $\sigma_{u,\max}/u_*$  for a wide range of relative roughness. Most of the data are from studies that were not designed for the purpose of assessing the effect of relative roughness on turbulence intensity. Instead, most workers showed vertical profiles  $\sigma_u/u_*$  for a limited range of relative roughness. We digitized these vertical profiles and extracted the peak near-bed value of  $\sigma_u/u_*$  for each experiment. The resultant data clearly show that the peak value in the turbulence intensity increases with decreasing relative roughness  $k_s/h$ . Figure 5 does not include data from the numerous studies that have measured

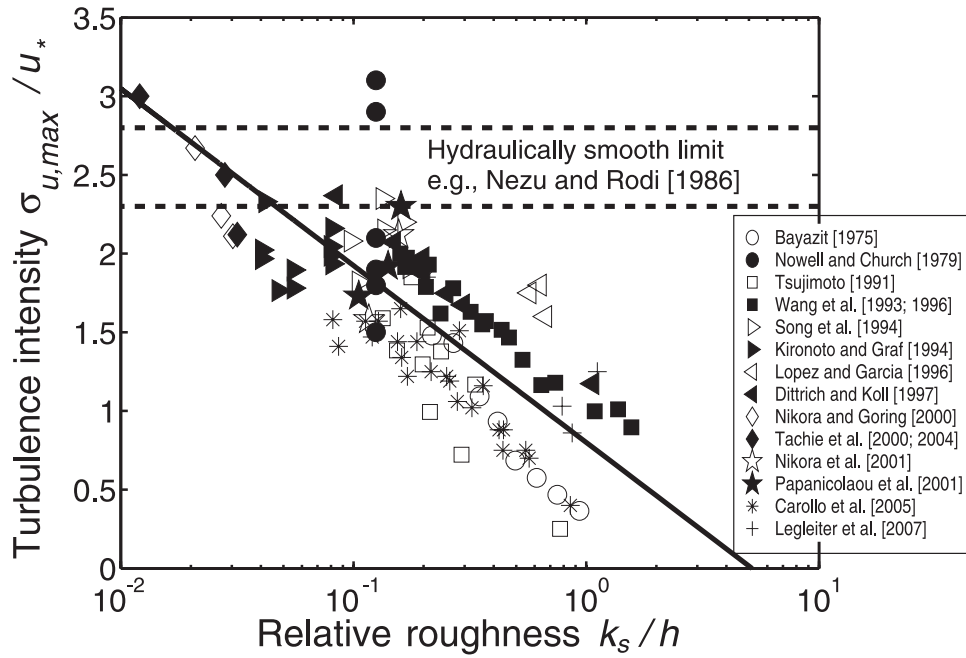


**Figure 5.** Near-bed peak turbulence intensity versus relative roughness. All points are data from previously published studies (see text for details). The two horizontal dashed lines represent the range in peak turbulent intensities for hydraulically smooth flow. The solid line is the model fit to the data with  $\alpha_2 = 0.2$  (equation (23)).

$\sigma_{u,\max}/u_*$  for hydraulically smooth flow. Most data for smooth beds, however, range from about 2.2 to 2.8 (as indicated by dashed lines on Figure 5) [e.g., *Nezu and Rodi*, 1986]. Almost all of the compiled data for flow over rough beds indicate smaller  $\sigma_{u,\max}/u_*$  than is typical for smooth-bed flows.

[44] The trend of increasing  $\sigma_{u,\max}/u_*$  with decreasing  $k_s/h$  in Figure 5 is significant despite the fact that the data cover a wide range of roughness types including boulders and gravel in natural streams [*Nikora and Goring*, 2000; *Legleiter et al.*, 2007], and gravel, spheres, wire mesh, and square blocks in laboratory flumes. The differences in roughness type, as well as differences in the spatial concentration of roughness elements on the bed, are probably the main reasons for scatter in the data. For example, the experiments of *Nowell and Church* [1979] were designed to assess variable concentrations of roughness elements with the same roughness length-scale (Lego blocks). We made no attempt to account for the effect of roughness concentration, therefore the data of *Nowell and Church* [1979] plot as a vertical line on Figure 5, with increasing  $\sigma_{u,\max}/u_*$  corresponding to lower areal roughness concentration. Their two experiments that have the largest values of  $\sigma_{u,\max}/u_*$  (and are the most significant outliers on Figure 5) had roughness concentrations of only  $\sim 0.01$  and  $0.02$ . It is likely that the parameter  $k_s/h$  significantly overestimates the actual roughness in these experiments due to the extremely low roughness concentrations used. If a roughness concentration correction were made, these points would be shifted to the left on Figure 5 (i.e., smaller  $k_s/h$ ) and would be more in line with the rest of the data.

[45] To our knowledge, a unified model for the turbulence intensity as a function of relative roughness has yet to be

proposed. We hypothesize that the reduction in turbulence intensity with increasing relative roughness is due to reduced macro-scale turbulent motions. For the same total shear stress, deeper flows are faster near the free surface, and therefore velocity fluctuations can be larger because the differential flow velocity across the total depth is greater. On the basis of the evidence for scaling of turbulent sweeps to the outer-flow variables (discussed above), it seems plausible that turbulence intensity also should scale with the depth-averaged flow velocity  $U$ , which in turn is a function of relative roughness. We therefore propose that

$$\frac{\sigma_{u,\max}}{u_*} = \alpha_2 \frac{U}{u_*} \quad (21)$$

where  $\alpha_2$  is a constant of proportionality between the depth-averaged velocity and the peak near-bed turbulence intensity.

[46] Many formulas have been proposed for the depth-averaged flow velocity of gravel bed rivers and steep streams. One of the most widely used is that of *Bathurst* [1985],

$$\frac{U}{u_*} = 5.62 \log\left(\frac{h}{k_s}\right) + 4. \quad (22)$$

Combining equations (21) and (22) results in a semi-empirical model for the peak turbulence intensity

$$\frac{\sigma_{u,\max}}{u_*} = \alpha_2 \left[ 5.62 \log\left(\frac{h}{k_s}\right) + 4 \right], \quad (23)$$

where, based on a best fit with data in Figure 5,  $\alpha_2 = 0.2$ . Thus the peak turbulent fluctuations are typically 20% of the depth-averaged velocity, and decrease with increasing relative roughness.

#### 4.8. Summary of Slope-Dependent Effects

[47] In summary, there are several potential mechanisms for the observed reduction in sediment mobility with increasing slope and relative roughness. These are variations in drag from channel walls and morphologic structures on the bed, friction angles, particle emergence, air entrainment, lift and drag coefficients, and the structure of the local velocity and turbulent fluctuations. Drag from channel walls and morphologic structures, as well as friction angles, might vary with channel slope in some natural streams due to changes in channel and bed morphology, but the dependency on slope is most likely negligible in flume experiments. Since, both laboratory and field measurements show approximately the same trend in  $\tau_{*c}$  with  $S$ , these factors alone cannot explain the data. Grain emergence and aeration are potentially important, but cannot explain the data for relatively low slopes. Lift and drag coefficients, unfortunately, are poorly known. The data that exist suggest that the drag coefficient increases with increasing slope due to backwater effects and an associated pressure differential, which would increase the mobility of particles on steeper slopes. This suggests, through a process of elimination, that the local flow velocity about the grains must decrease with increasing slope. Indeed, experimental studies have shown that, for the same bed shear stress, both the average local velocity and the magnitude of near-bed turbulent velocity fluctuations tend to decrease with increasing slope. These effects appear to be due to variations in the vertical structure of mixing (i.e., the eddy viscosity) and large-scale turbulent motions as a result of changes in relative roughness.

### 5. Model Evaluation and Results

[48] In order to explore the potential slope-dependent effects quantitatively,  $\tau_{*cT}$  is calculated as a function of bed slope following equation (12). Equation (12) is solved using a simple iterative numerical scheme since bed slope appears on both sides of the equation. For a given total shear stress and channel slope, flow depth is solved from equation (11). The ratio of the lift force to the drag force is set to  $F_L/F_D = 0.85$  [Chepil, 1958; Wiberg and Smith, 1987a]. Since much of the data in Figure 1 have been corrected for wall drag, we set  $\tau_w = 0$  in equation (12), which makes equations (12) and (13) equivalent (i.e.,  $\tau_{*cT} = \tau_{*cTR}$ ). The component of the total stress spent on drag from morphologic structures ( $\tau_m$ ) initially is set to zero for simplicity, since it is unlikely to contribute to a slope dependence as discussed in section 4.2. The sensitivity of the model to morphologic drag is discussed in section 7. The submerged specific density of sediment is set to  $r = 1.65$  for siliceous material. The friction angle is initially set to  $60^\circ$  for the case of  $D \cong k_s$  [Wiberg and Smith, 1987a]. The sensitivity to different friction angles and a heterogeneous grain-size distribution are considered in section 6. Only coarse sediment is considered, so that viscous effects are neglected and  $C_D = 0.9$  [Nelson et al., 2001; Schmeckle

et al., 2007]. Spherical particles are assumed, and the cross-sectional area of the particle that is exposed to the flow  $A_{xs}$  and the submerged volume of the particle  $V_{ps}$  are given in Appendix A. First we discuss the baseline log-profile model and then systematically include particle emergence, flow aeration, the quadratic velocity profile, and turbulent fluctuations.

#### 5.1. Baseline Log-Profile Model

[49] Initially, equation (12) is solved by neglecting all of the slope-dependent effects discussed above and therefore is similar to the model presented by Wiberg and Smith [1987a]. The logarithmic velocity profile (equation (16)) was squared and integrated from  $z_0 \leq z \leq D$  and combined with equation (12). As shown in Figure 6, the log-profile model predicts a relatively constant value of  $\tau_{*cT}$  for low channel slopes that decreases rapidly at high channel slopes. This trend is expected from inspection of equation (12), as the channel slope approaches the friction angle,  $\tau_{*cT}$  tends to zero. This model does not match the data well.

#### 5.2. Particle Emergence

[50] Including particle emergence produces the exact same trend as the baseline log-profile model, except for channel slopes greater than about 0.05 where  $\tau_{*cT}$  abruptly increases as particles emerge from the flow (Figure 6). Again, at very high slopes  $\tau_{*cT}$  is forced to zero where the channel slope equals the friction angle. The dashed line in Figure 6 separates the regions of particle submergence ( $D < h$ ) and emergence ( $D > h$ ).

#### 5.3. Flow Aeration

[51] The effective density of the water-air mixture was calculated using equations (14) and (15). As mentioned above, equation (15) should provide a minimum estimate of aeration. Flow aeration has little affect for channel slopes less than 0.01 (Figure 6). In the region of  $0.01 < S < 0.05$  flow aeration tends to offset the gravitational effects in the baseline log-profile model, resulting in a more constant value of  $\tau_{*cT}$ . For channel slopes greater than 0.05, aeration causes a slightly greater  $\tau_{*cT}$ , but the model prediction is dominated by the effect of emergence at these large slopes.

#### 5.4. Quadratic Velocity Profile

[52] The effects of wake mixing on the eddy viscosity is introduced in the model by using the quadratic velocity profile (equation (20)), rather than the log profile (equation (16)). By including the quadratic velocity profile, particles on all slopes are predicted to be less mobile and hence the Shields curve is shifted upwards. This is because the quadratic profile predicts lower velocities than the log profile at all channel slopes (Figure 4). Importantly, including the quadratic profile results in an increasing critical Shields stress with slope in the region of particle submergence. This also results in a smoother transition from fully submerged to partially emerged grains.

#### 5.5. Turbulent Fluctuations

[53] Sediment is most likely to be entrained when turbulent fluctuations act to increase the local velocity around the grains above the average velocity. These downstream directed turbulent fluctuations, therefore, are included in the

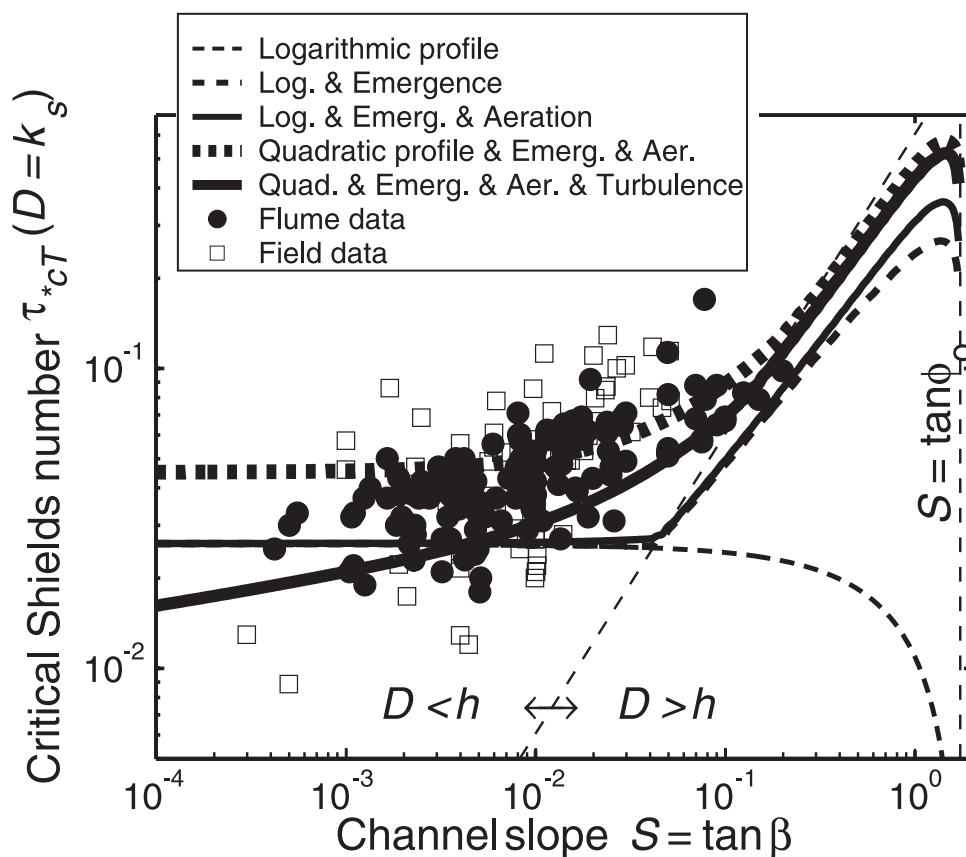


**Figure 6.** Model predictions and data for critical Shields stress as a function of channel slope. The effects considered include: (1) logarithmic velocity profile, (2) particle emergence, (3) flow aeration, (4) quadratic velocity profile, and (5) turbulent fluctuations. These are included cumulatively, such that the thick solid line represents all of the effects. The dashed diagonal line separates the fields of particle submergence ( $D < h$ ) from emergence ( $D > h$ ). The model predicts  $\tau_{*cT} = 0$  where the bed-slope angle equals the friction angle, indicated by the vertical dashed line. Note that the predictions for  $S > 0.57$  should not be deemed reliable, as these slope angles ( $>30$  degrees) are larger than the typical angle of repose of loose sediment. Data shown are the same as Figure 1.

model by equating the local velocity  $u(z)$  in equation (12) to an effective entrainment velocity, which is the sum of the local average velocity  $\bar{u}(z)$  and the magnitude of turbulent excursions  $\sigma_{u,\max}$  (i.e.,  $u(z) = \bar{u}(z) + \sigma_{u,\max}$ ). For simplicity,  $\sigma_{u,\max}$  is assumed to be uniform about the exposed cross-sectional area of the particle  $A_{xs}$  and is given by equation (23) with  $\alpha_2 = 0.2$ .

[54] The model indicates that turbulent fluctuations affect incipient motion significantly. First, fluctuations increase the drag and lift forces on the particle, so that mobility is increased (i.e.,  $\tau_{*cT}$  is decreased) for all channel slopes (Figure 6). Second, the magnitude of the fluctuations are much larger for lower slopes (deeper flows), which results in a significant increase in  $\tau_{*cT}$  with increasing channel slope. The result is a model that reproduces the trend and the magnitude of the data well.

### 5.6. Summary of Model Results

[55] The baseline log-profile model does not predict the empirical trend of increasing  $\tau_{*cT}$  with channel slope; in fact, it predicts an opposite trend. In light of this, the additional components considered here are a considerable

improvement. Aeration has the least affect on the trend of the data. Particle emergence is significant, but only for slopes greater than 0.05. The most important effects considered are changes to the local velocity profile due to an eddy viscosity that incorporates wake mixing and changes to the intensity of velocity fluctuations due to the relative roughness dependency of macro-scale turbulence.

### 6. Mixed Particle Sizes

[56] Thus far uniform-size sediment (or  $D = k_s$ ) has been assumed. A more complete model must include heterogeneous particle sizes. Mixed particle sizes can lead to important dynamics in gravel and boulder-bedded streams, such as particle clustering and size-selective transport [Paola *et al.*, 1992; Wilcock and McArdeell, 1993; Church and Hassan, 2002; Yager *et al.*, 2007]. Assessing these processes in a rigorous way is beyond the scope of this paper. Here we take the simplistic approach of treating multiple grain sizes through the friction angle term in equation (12), which is dominantly a function of the particle size of interest  $D$  relative to the roughness length scale of

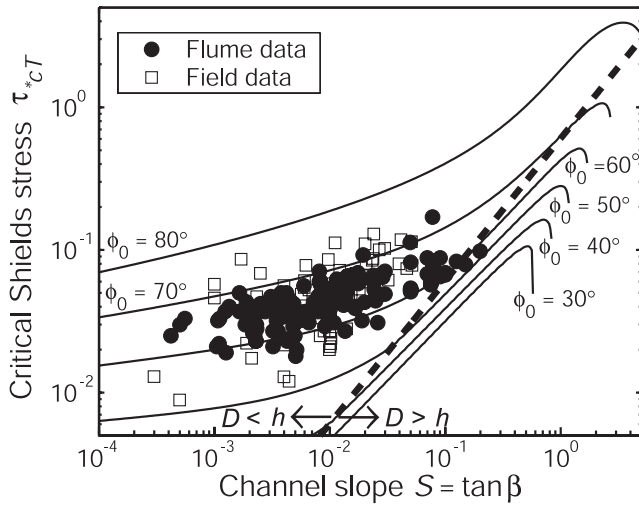


**Figure 7.** Model predications of the critical Shields stress versus slope for different values of the friction angle  $\phi_0$ . The model includes particle emergence, flow aeration, the quadratic velocity profile, and turbulent fluctuations. The dashed diagonal line separates the fields of particle submergence ( $D < h$ ) from emergence ( $D > h$ ). Each model prediction tends to zero at large slopes where the bed-slope angle equals the friction angle. Data shown are the same as Figure 1.

the bed  $k_s$  [Kirchner et al., 1990; Johnston et al., 1998]. Wiberg and Smith [1987a] proposed the geometric relation

$$\phi_0 = \cos^{-1} \left[ \frac{D/k_s + z^*}{D/k_s + 1} \right] \quad (24)$$

based on the data of Miller and Byrne [1966], where  $k_s$  is the median particle size (i.e.,  $k_s = D_{50}$ ) and  $z^*$  is the “average level of the bottom of the almost moving grain” and was found empirically to be  $z^* = -0.02$  for natural sand [Wiberg and Smith, 1987a].

[57] Multiple Shields curves were generated for different friction angles from equations (12) and (24) (Figure 7). Particles are more difficult to move for larger friction angles, which results in an upward shift of the Shields curve. When  $D/k_s$  is unity, the friction angle given by equation (24) is predicted to be  $\phi_0 \approx 60^\circ$ , which is consistent with the previous calculations (i.e., Figure 6). More recent work on gravel beds have found  $\phi_0 \approx 52^\circ$  for  $D/k_s = 1$  [Buffington et al., 1992; Johnston et al., 1998]. It also has been shown that friction angles can vary substantially for the same value of  $D/k_s$  due to variable pocket geometries [Kirchner et al., 1990]. Thus it might be more appropriate to use a friction angle that is smaller than the mean angle predicted by equation (24). As shown in Figure 7, however, the data are consistent with friction angles ranging from about  $60^\circ$  to  $70^\circ$ . This suggests that using a mean friction angle (e.g., equation (24)) is reasonable. We have adopted equation (24) over other empirical power law relations to be consistent with previous modeling work [Wiberg and Smith, 1987a].

[58] To predict the sizes of grains that are most mobile for a given boundary shear stress, it is useful to normalize the

critical shear stress by  $k_s$ , rather than  $D$ , because  $k_s$  is constant for a bed composed of multiple grain sizes [e.g., Wiberg and Smith, 1987a]. The curves for different friction angles in Figure 7 are interpreted to represent different relative particle sizes  $D/k_s$  following equation (24). Hence large friction angles are interpreted to be for particles with small  $D/k_s$  and small friction angles are interpreted to be for particles with large  $D/k_s$ . Figure 8 shows that the theoretical Shields curves collapse when normalized by  $k_s$  (i.e.,  $(D/k_s) \tau^*_{cT}$ ), which indicates that the critical shear stress necessary to mobilize different sediment sizes does not vary significantly (typically less than a factor of three). Moreover, the relative mobility of different sizes is a complex function of channel slope.

[59] This is clearer in Figure 9 where the critical shear stress is plotted versus the relative particle size [cf. Wiberg and Smith, 1987a]. Here the critical shear stress needed to move a given size  $D$  is normalized by the value needed to move the size  $D = k_s$ , where, following Wiberg and Smith [1987a],  $k_s$  is interpreted to be the median particle size. Thus particle sizes that are more difficult to move than  $D = k_s$  have values greater than unity and particles that are easier to move have values less than unity. A horizontal line represents equal mobility – where all particle sizes move at the same shear stress. For most channel slopes and particle sizes, the model predicts near equal mobility for the fine fraction  $D < k_s$ . The coarse fraction, on the other hand, is predicted to be the most mobile sediment on low slopes ( $S < 0.01$ ), the least mobile sediment on steep slopes ( $S > 0.05$ ), and approximately as mobile as the finer material on the moderate slopes in between. The latter finding is consistent with most studies, which have shown that sediment is nearly equally mobile, since many gravel bed rivers studied have moderate slopes around 0.02 [e.g., Parker, 1990; Parker et al., 2007]. The large values of relative shear stress for the coarse fraction on steep slopes is also consis-

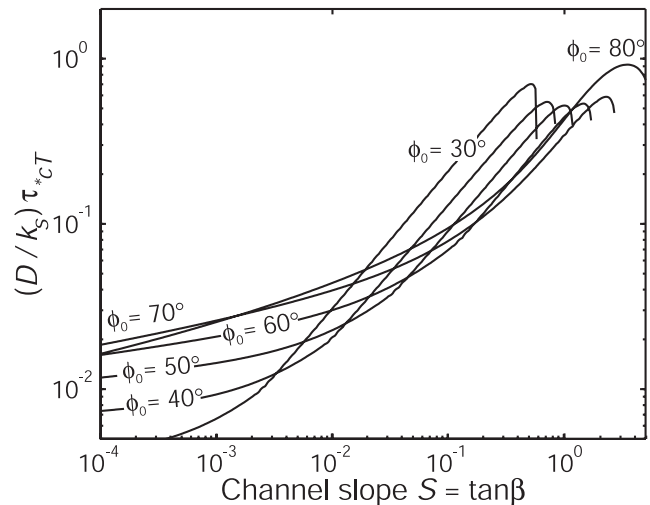


**Figure 8.** Same as Figure 7 except that the critical shear stress needed to move particle size  $D$  is normalized by  $k_s$ , which is constant for a bed of multiple particle sizes and represents here the median particle size on the bed. Thus the curves indicate the relative mobility of different particle sizes under the same shear stress. The relationship between  $D$ ,  $k_s$ , and  $\phi_0$  is given by equation (24).

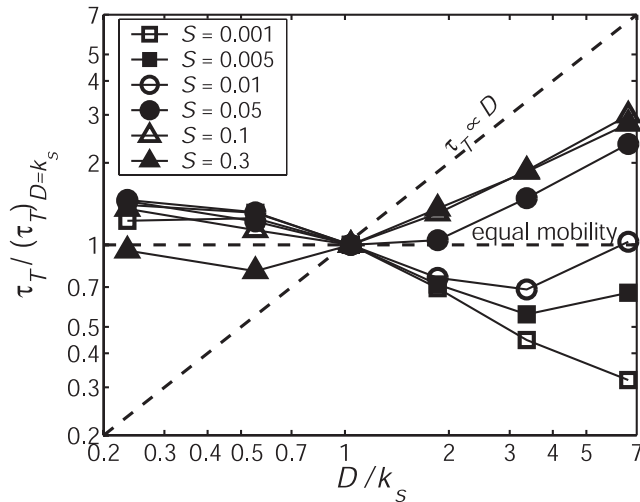


**Figure 9.** Total shear stress at incipient motion of particle size  $D$  normalized by the total shear stress necessary to move particle size  $D = k_s$ , versus the relative particle size  $D/k_s$ . Here,  $k_s$  represents the median particle size on the bed. The horizontal dashed line represents equal mobility. The diagonal dashed line represents size-selective transport given by the Shields stress, where the critical stress is proportional to the particle size.

tent with observations that boulders are relatively immobile in mountain streams [e.g., *Yager et al.*, 2007]. The reason for the systematic increase in relative shear stress with  $S$  for the coarser fraction is primarily because large particles become emergent from the flow before smaller particles, rendering them less mobile.

[60] The force balance model described here provides a straightforward method of predicting relative mobility of a mixed bed. These predictions, however, should be treated with caution. For example, on very low slopes ( $S < 10^{-2}$ ) the model predicts that coarse particles will move before finer particles (Figure 9). This is because the increased weight of larger particles is more than compensated for by smaller friction angles, which renders coarser particles more mobile. While this tendency has been documented before [*Solari and Parker*, 2000; *Brummer and Montgomery*, 2003], size-selective mobility favoring finer sediment is typically considered the norm [e.g., *Parker*, 1990; *Buffington et al.*, 1992; *Paola et al.*, 1992; *Powell et al.*, 2001; *Ferguson*, 2003]. Others have found similar results as our model and argued that shifting of coarser particles could allow rapid entrainment of finer sediment [*Kirchner et al.*, 1990], or coarser particles might be partially buried by fines [*Buffington et al.*, 1992], rendering mixtures more equally mobile than simple models predict. We caution that changes to the empirical coefficients used to model aeration, wake mixing, and turbulent fluctuations would alter the overlap between the Shields curves in Figure 8, which could affect the predictions of size-selective mobility.

## 7. Discussion

### 7.1. Drag From Morphologic Structures

[61] In the calculations above, the magnitude of stress spent on morphologic structures was set to zero ( $\tau_m = 0$ ) for

simplicity. While it was argued in section 4.2 that morphologic drag appears to be independent of channel-bed slope, it is probable that the magnitude of drag due to protruding particles, particle clusters and larger morphologic structures is non-negligible in flume experiments and natural streams [e.g., *Millar*, 1999]. We calculated the critical Shields stress as a function of slope using equation (12) with  $\phi_0 = 60^\circ$  for constant values of the ratio of morphologic drag to the total stress ( $\tau_m/\tau_T$ ). As expected, including a constant value of  $\tau_m/\tau_T$  (i.e., one that does not trend with channel slope) changes the magnitude of the critical Shields stress for a given slope (Figure 10). Increasing  $\tau_m$  causes an increase in  $\tau_{*cT}$  because a smaller portion of the total stress is available to move sediment. The model fits the data well if morphologic drag is set between 0 and 60% of the total driving stress. Larger portions of drag (e.g., 80%) result in an over-prediction of the data. This estimated range in morphologic drag is consistent with estimates by *Parker et al.* [2007] that morphologic form drag typically ranges from 21% to 57% of the total driving stress, based on a compilation of bankfull hydraulic measurements from gravel bed rivers.

[62] In order to make the model easier to apply, we have fit expressions to the theoretical curves in Figure 10 for  $\tau_m/\tau_T = 0\%$ , 40%, and 60%. It was found that 4<sup>th</sup>-order polynomials approximate well the theoretical curves for  $10^{-4} < S < 0.5$ :

$$\tau_{*cT} = \exp[P_4 X^4 + P_3 X^3 + P_2 X^2 + P_1 X + P_0] \quad (25)$$

where  $X = 0.407 \ln(142S)$  after performing a centering and scaling algorithm to improve the least squares fit.  $P_0$ ,  $P_1$ ,  $P_2$ ,  $P_3$  and  $P_4$  are constants given by  $-3.57$ ,  $0.476$ ,  $0.199$ ,  $0.107$ , and  $2.49 \times 10^{-2}$  respectively for  $\tau_m/\tau_T = 0\%$ ;  $-3.14$ ,  $0.410$ ,  $0.142$ ,  $8.94 \times 10^{-2}$ , and  $2.59 \times 10^{-2}$  respectively for  $\tau_m/\tau_T = 40\%$ ; and  $-2.8$ ,  $0.377$ ,  $0.121$ ,  $7.44 \times 10^{-2}$ , and  $2.02 \times 10^{-2}$  respectively for  $\tau_m/\tau_T = 60\%$ . The errors for these approximate curves are less than the thickness of the lines on Figure 10 within the regime  $10^{-4} < S < 0.5$ .

### 7.2. Predicting Bed-Surface Grain Size

[63] Many river restoration efforts attempt to adjust bed-surface particle size to improve habitat (e.g., for salmonid spawning) [*Kondolf and Wolman*, 1993]. Over long time-scales, it is commonly assumed that particle sizes on the channel bed are adjusted to the hydraulic conditions, so that the bankfull Shields stress  $\tau_{*bf}$  is approximately equal to the critical Shields stress  $\tau_{*cT}$  [*Parker*, 1978; *Andrews*, 1983]. While oversimplified, such an assumption is powerful as it allows for a simple prediction of bed surface sediment size [e.g., *Buffington et al.*, 2004]. *Buffington and Montgomery* [1999] collected data from several stream reaches with different morphologies to test the assumption that  $\tau_{*bf} \approx \tau_{*cT}$ . They found that particle sizes were substantially finer than expected (i.e.,  $\tau_{*bf} > \tau_{*cT}$ ), which they attributed to morphologic form drag. This conclusion was supported by the fact that reaches with more woody debris had larger  $\tau_{*bf}$ , as shown in Figure 11. Their data also show, however, that for a given channel morphology (with presumably similar values of morphologic drag),  $\tau_{*bf}$  systematically increases with channel slope and systematically deviates from the assumed  $\tau_{*cT} = 0.03$  (Figure 11). The increase in  $\tau_{*bf}$  with

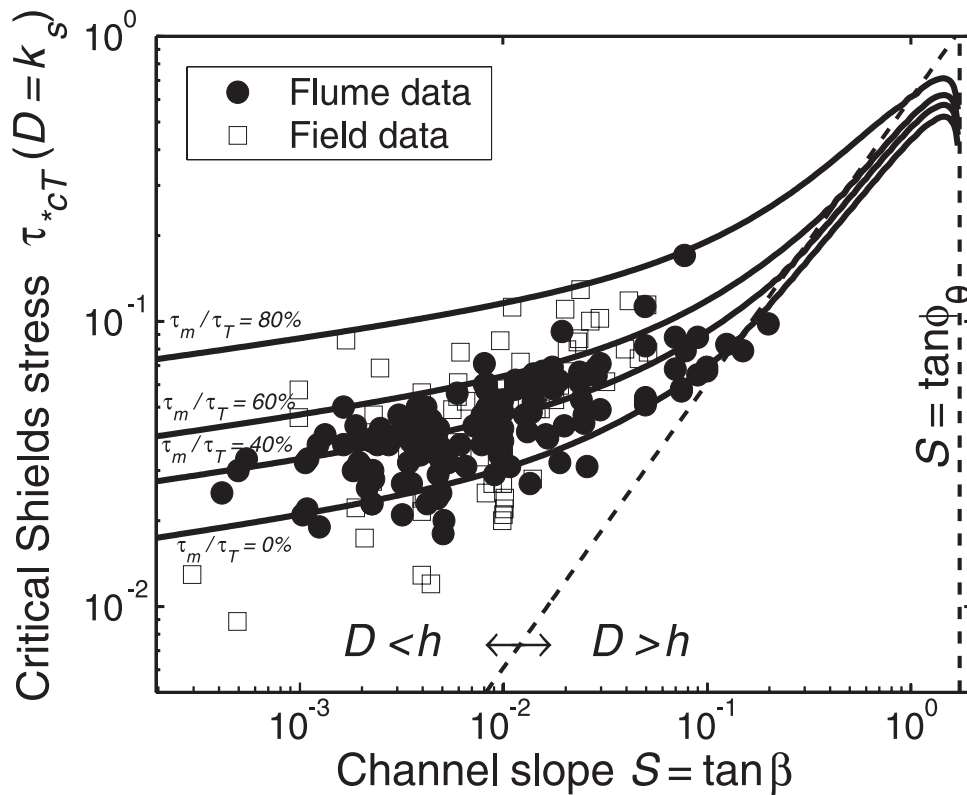


**Figure 10.** Model predications of the critical Shields stress versus slope for different values of the ratio of the stress borne by morphologic structures to the total stress  $\tau_m/\tau_T$ . The model includes particle emergence, flow aeration, the quadratic velocity profile, and turbulent fluctuations. The dashed diagonal line separates the fields of particle submergence ( $D < h$ ) from emergence ( $D > h$ ). Each model prediction tends to zero at large slopes where the bed-slope angle equals the friction angle. Data shown are the same as Figure 1.

$S$  is consistent with our model. Figure 11 shows the model predictions (equation (12)) for different ratios of morphologic drag to the total stress. The model predictions are an improvement over assuming  $\tau_{*cT} = 0.03$ , but still underestimate the data trend of increasing  $\tau_{*bf}$  with  $S$ . This could be due to systematic variations in drag or friction angles within each morphologic division, among other assumptions inherent in such an analysis [Buffington and Montgomery, 2001; Millar and Rennie, 2001; Wilcock, 2001]. The model predicts that the plane bed reaches have morphologic drag that constitutes zero to 60% of the total stress. In the wood-poor, pool-riffle reaches, morphologic drag is predicted to be about 60 to 80% of the total stress, and many of the wood-rich, pool-riffle reaches appear to have greater than 80% morphologic drag. These results are consistent with field measurements and analysis by Buffington [1998, Chapter 3].

[64] Most rivers networks tend to have finer sediment on their beds in the downstream direction. This is typically attributed to abrasion of particles, selective transport of finer sediment, or a downstream reduction in shear stress. Some workers, however, have found that particle size increases in the downstream direction [Solari and Parker, 2000; Brummer and Montgomery, 2003]. Our study offers an explanation for this counter intuitive finding. If  $\tau_{*cT}$  decreases downstream (because  $S$  decreases) more rapidly

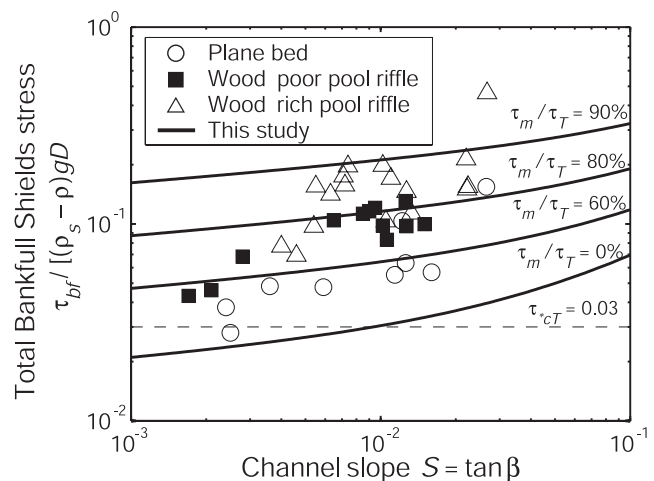


**Figure 11.** Field measurements of total bankfull Shields stress versus channel slope from Buffington and Montgomery [1999]. The data are stratified according to channel morphology. The dashed line represents the predicted relation where  $\tau_{*cT} = 0.03$ , as assumed by Buffington and Montgomery [1999]. The solid lines are the expected relations using our model (equation (12)) for different percentages of stress borne by morphologic structures divided by the total stress ( $\tau_m/\tau_T$ ).

than the bankfull shear stress decreases, then the equilibrium particle size is predicted to increase downstream (if  $\tau_{*bf} \approx \tau_{*cT}$ ). One then might expect to find downstream coarsening in steep headwater channels, since  $\tau_{*cT}$  varies most strongly with slope for large slopes (Figure 6), which is consistent with the observations of *Brummer and Montgomery* [2003].

### 7.3. Implications for Low and High Gradient Channels

[65] In lowland gravel bed rivers, equation (12) indicates that  $\tau_{*cT}$  can be a factor of two smaller than 0.03. In most natural settings, these low sloping rivers could have substantial concentrations of sand on the bed. The model of *Wilcock and Crowe* [2003], based on the experiments of *Wilcock et al.* [2001], shows that sand can cause a reduction in  $\tau_{*cT}$  from about 0.035 to 0.02 where the sand fraction increases from 10% to 30%. These workers also report a systematic reduction in channel slope with increasing sand content (from about  $8 \times 10^{-3}$  to  $1.4 \times 10^{-3}$ ). Our model predicts a similar reduction in  $\tau_{*cT}$  for this range in slopes due to enhanced near-bed average velocities and turbulent fluctuations, without regard to sand content (Figure 6). More work is needed to sort out the potential overlapping influences of sand content and channel slope on incipient motion.

[66] Most of the river network in hilly and mountainous landscapes is composed of small, steep channels, which are typically mantled by coarse sediment. The transport of boulders is considered a rate limiting process for bedrock erosion [*Seidl et al.*, 1994; *Sklar and Dietrich*, 2004; *Lamb et al.*, 2006] and has been shown to set the concavity of the longitudinal profile [*Sklar and Dietrich*, 2006]. It is common to assume that boulder transport on slopes  $> 0.1$  occurs only by debris flows [*Stock and Dietrich*, 2003], or that boulders must break down in place. Moreover, stream-restoration researchers now place boulder clusters or other roughness elements in steep streams in an attempt to capture and store sediment to restore quasi-natural conditions [*Rosgen*, 1996; *Stallman et al.*, 2004]. These efforts are hampered because application of a constant  $\tau_{*c}$  in mountain streams has had little success [e.g., *Zimmermann and Church*, 2001]. Our study allows for quantitative field estimation of boulder transport by fluvial processes. Equation (12) indicates that boulders become increasingly difficult to move by fluvial processes with increasing slope – but not impossible, as long as there is sufficient flow and boundary shear stress.

[67] Also of note is the possibility that the peak in the critical Shields stress (Figure 10) identifies a zone of channel slopes in which sediment transport converges, which could be important for debris flow initiation. At very large slopes that approach the friction angle, sediment is highly mobile due to the large gravitational force pulling particles downslope. Particles that are transported in these steep zones by overland flow or raveling [e.g., *Imaizumi et al.*, 2006] might collect at lower slopes where particles are relatively immobile (i.e., for slopes of about  $0.2 < S < \tan \phi_0$ ), which could eventually lead to failure initiating debris flows.

## 8. Conclusions

[68] The critical Shields stress for incipient motion of sediment in open-channel flow increases with channel

slope. This observation is contrary to standard theoretical models for incipient motion that predict increased mobility with increasing channel slope due to the added gravitational force in the downstream direction. Several processes might explain this discrepancy including variable drag caused by morphologic structures, wall drag, friction angles, grain emergence, flow aeration, changes to the vertical structure of flow velocity, and turbulent fluctuations. Increasing friction angles and drag due to changes in bed morphology do not appear to be the cause of the slope dependency, as is often assumed, because significant changes in bed morphology in controlled flume experiments seems unlikely. Moreover, data from flume experiments and natural streams are not significantly different, which suggests that other processes are responsible for the slope-dependent critical Shields stress. A simple 1-D force-balance model indicates that the effect of aeration is small, and that grain emergence cannot explain the trend in the data for low slopes ( $S < 0.1$ ). Through a process of elimination, it is concluded that the local velocity about the grains must decrease with increasing channel slope, for the same shear stress and particle size. A quadratic profile for the average local velocity is proposed based on a 1-D eddy viscosity model where mixing is dominated by wakes shed by particles. Inclusion of this profile in the force balance improves the model predictions of the trend in the data. To include the fluctuating component of local velocity due to turbulence, we hypothesize that the intensity of near-bed turbulent fluctuations are proportional to the depth-averaged flow velocity. A compilation of data supports this hypothesis and reveals the proportionality constant to be  $\sim 0.2$ . The combined effects of particle emergence, an eddy viscosity that incorporates wake mixing, and turbulent fluctuations in the model produce increasing  $\tau_{*cT}$  with increasing slope that match the available data well. Collectively, these effects arise because of the coincident change in relative roughness with slope, since flow depth is inversely related to channel slope for a given bed-shear stress and particle size. Extension to multiple grain sizes indicates that the coarse fraction becomes increasingly less mobile on steeper slopes, primarily due to particle emergence. A slope-dependent critical Shields stress has broad implications as the assumption of constant  $\tau_{*c}$  is the basis of many models used to predict such things as bed load transport, debris flow entrainment, bedrock erosion, downstream fining, and bed particle size.

## Appendix A

[69] The cross-sectional area of the particle that is exposed to the flow  $A_{xs}$  and the volume of the particle during partial emergence  $V_{ps}$  are calculated by integrating a partial sphere. Let  $h^* = h/D$  and  $z_0^* = z_0/D$ .  $A_{xs}$  is given by

$$\frac{A_{xs}}{D^2} = \left[ \left( h^* - \frac{1}{2} \right) \sqrt{h^* - h^{*2}} + \frac{1}{4} \arcsin(2h^* - 1) - \left( z_0^* - \frac{1}{2} \right) \cdot \sqrt{z_0^* - z_0^{*2}} - \frac{1}{4} \arcsin(2z_0^* - 1) \right] \text{ for } h^* < 1 \quad (\text{A1})$$

and does not include the portion of the particle that is below  $z_0$  or above  $h$ . No account of shielding due to grain packing

or burial are taken into account except through the term  $z_0$ . When a particle is fully submerged  $A_{xs}$  is given by

$$\frac{A_{xs}}{D^2} = \left[ \frac{\pi}{8} - \left( z_0^* - \frac{1}{2} \right) \sqrt{z_0^* - z_0^{*2}} - \frac{1}{4} \arcsin(2z_0^* - 1) \right] \quad \text{for } h^* \geq 1 \quad (\text{A2})$$

The partially submerged volume of a particle  $V_{ps}$  is given by

$$\frac{V_{ps}}{D^3} = \pi h^{*2} \left( \frac{1}{2} - \frac{1}{3} h^* \right) \quad \text{for } h^* < 1 \quad (\text{A3})$$

For a fully submerged sphere ( $h^* \geq 1$ )  $V_{ps} = V_p = 1/6\pi D^3$ . More detail on these integrations can be found by Yager et al. [2007].

[70] **Acknowledgments.** This study was funded by NASA BioMars and the National Center for Earth Surface Dynamics. We thank Elowyn Yager for enlightening discussions about steep channels. The manuscript has benefited by the constructive reviews of D. Rickenmann and J. Buffington.

## References

- Aberle, J., and G. M. Smart (2003), The influence of roughness structure on flow resistance on steep slopes, *J. Hydraul. Res.*, 41(3), 259–269.
- Aguirre-Pe, J. (1975), Incipient erosion in high gradient open channel flow with artificial roughness elements, *Proc. 16th Congr. Int. Assoc. Hydraul. Res. San Paulo Brazil*, 2, 137–180.
- Aguirre-Pe, J., and R. Fuentes (1991), Movement of big particles in steep, macro-rough streams, *Proc. 24th Congr. Int. Assoc. Hydraul. Res. Madrid, Spain*, A, 149–158.
- Aguirre-Pe, J., M. L. Olivero, and A. T. Moncada (2003), Particle densimetric froude number for estimating sediment transport, *J. Hydraul. Eng. Asce*, 428–437.
- Aivazyan, O. M. (1987), Stabilized aeration on chutes, in *Hydrotechnical Construction*, pp. 713–722, Plenum Press, New York.
- Andrews, E. D. (1983), Entrainment of gravel from naturally sorted riverbed material, *Geol. Soc. Am. Bull.*, 94, 1225–1231.
- Armanini, A., and C. Gregoretti (2005), Incipient sediment motion at high slopes in uniform flow conditions, *Water Resour. Res.*, 41, W12431, doi:10.1029/2005WR004001.
- Ashida, K., and M. Bayazit (1973), Initiation of motion and roughness of flows in steep channels, *Int. Assoc. Hydraul. Res., Proc. 15th Congress, Istanbul, Turkey*, 1, 475–484.
- Ashworth, P. J., and R. I. Ferguson (1989), Size-selective entrainment of bed-load in gravel bed breams, *Water Resour. Res.*, 25(4), 627–634.
- Ashworth, P. J., R. I. Ferguson, P. E. Ashmore, C. Paola, D. M. Powell, and K. L. Prestegard (1992), Measurements in a braided river chute and lobe: 2. Sorting of bed-load during entrainment, transport, and deposition, *Water Resour. Res.*, 28(7), 1887–1896.
- Bartnick, W. (1991), Determination of the critical conditions of incipient motion of bed load in mountain rivers, in *Fluvial Hydraulics in Mountain Regions*, edited by A. Armanini, and G. Di Silvio, pp. 83–88, Springer-Verlag, Berlin.
- Batchelor, G. K. (1967), *An Introduction to Fluid Dynamics*, 615 pp., Cambridge University Press, Cambridge.
- Bathurst, J. C. (1985), Flow resistance estimation in mountain rivers, *J. Hydraul. Eng.*, 111(4), 625–643.
- Bathurst, J. C. (1987), Critical conditions for bed material movement in steep, boulder-bed streams, in *Erosion and Sedimentation in the Pacific Rim, Proceedings of the Corvallis Symposium, IAHS Publication no 165*, pp. 309–318.
- Bathurst, J. C., R. M. Li, and D. B. Simons (1979), *Hydraulics of Mountain Rivers*, 229 pp., Engineering Research Center, Colorado State University, Fort Collins, CO.
- Bathurst, J. C., H. H. Cao, and W. H. Graf (1984), *Hydraulics and Sediment Transport in a Steep Flume. Data from the EPFL Study, Report 64*, Inst. of Hydrol., Wallingford, Oxon, England.
- Bathurst, J. C., W. H. Graf, and H. H. Cao (1987), Bed load discharge equations for steep mountain rivers, in *Sediment Transport in Gravel-Bed Rivers*, edited by C. R. Thorne, J. C. Bathurst, and R. D. Hey, pp. 453–491, John Wiley & Sons.
- Bayazit, M. (1975), Free surface flow in a channel of large relative roughness, *J. Hydraul. Res.*, 14(2), 115–126.
- Bayazit, M. (1978), Scour of bed material in very rough channels, *J. Hydraul. Div.*, 104(HY9), 1345–1349.
- Best, J. L. (1992), On the entrainment of sediment and initiation of bed defects: insights from recent developments within turbulent boundary layer research, *Sedimentology*, 39, 797–811.
- Bettess, R. (1984), Initiation of sediment transport in gravel streams, *Proc. Inst. Civ. Eng.*, 77(Technical Note 407), 79–88.
- Braudrick, C. A., and G. E. Grant (2000), When do logs move in rivers?, *Water Resour. Res.*, 36(2), 571–583.
- Brayshaw, A. C., L. E. Frostick, and I. Reid (1983), The hydrodynamics of particle clusters and sediment entrainment in coarse Alluvial Channels, *Sedimentology*, 30(1), 137–143.
- Bridge, J. S., and S. J. Bennett (1992), A model for the entrainment and transport of sediment grains of mixed sizes, shapes, and densities, *Water Resour. Res.*, 28(2), 337–363.
- Brummer, C. J., and D. R. Montgomery (2003), Downstream coarsening in headwater channels, *Water Resour. Res.*, 39(10), 1294, doi:10.1029/2003WR001981.
- Buffington, J. M. (1998), The use of streambed texture to interpret physical and biological conditions at watershed, reach, and subreach scales, Ph.D. dissertation, University of Washington, 147 pp.
- Buffington, J. M., and D. R. Montgomery (1997), A systematic study of eight decades of incipient motion studies, with special reference to gravel-bedded rivers, *Water Resour. Res.*, 33(8), 1993–2029.
- Buffington, J. M., and D. R. Montgomery (1999), Effect of hydraulic roughness on surface textures of gravel-bed rivers, *Water Resour. Res.*, 35(11), 3507–3521.
- Buffington, J. M., and D. R. Montgomery (2001), Comment on “Effects of hydraulic roughness on surface textures of gravel-bed rivers” by John M. Buffington and David R. Montgomery - Reply, *Water Resour. Res.*, 37(5), 1529–1533.
- Buffington, J. M., W. E. Dietrich, and J. W. Kirchner (1992), Friction angle measurements on a naturally formed gravel stream bed: Implications for critical boundary shear stress, *Water Resour. Res.*, 28(2), 411–425.
- Buffington, J. M., D. R. Montgomery, and H. M. Greenberg (2004), Basin-scale availability of salmonid spawning gravel as influenced by channel type and hydraulic roughness in mountain catchments, *Can. J. Fish. Aquat. Sci.*, 61(11), 2085–2096.
- Burr, D. M., J. P. Emery, R. D. Lorenz, G. C. Collins, and P. A. Carling (2006), Sediment transport by liquid surficial flow: Application to Titan, *Icarus*, 181(1), 235–242.
- Byrd, T. C., and D. J. Furbish (2000), Magnitude of deviatoric terms in vertically averaged flow equations, *Earth Surf. Processes Landforms*, 25, 319–328.
- Carling, P. A. (1983), Threshold of coarse sediment transport in broad and narrow natural streams, *Earth Surf. Processes Landforms*, 8, 1–18.
- Carling, P. A., M. Hoffman, and A. S. Blatter (2002), Initial motion of boulders in bedrock channels, in *Ancient Floods, Modern Hazards: Principles and Applications of Paleoflood Hydrology*, American Geophysical Union, Washington, DC.
- Carollo, F. G., V. Ferro, and D. Termini (2005), Analyzing turbulence intensity in gravel bed channels, *J. Hydraul. Eng.*, 131(12), 1050–1061.
- Chang, H. H. (1998), Riprap stability on steep slopes, *Int. J. Sediment Res.*, 13(2), 40–49.
- Chanson, H. (1994), Air-water-interface area in self-aerated flows, *Water Res.*, 28(4), 923–929.
- Chanson, H. (2004), Drag reduction in skimming flow on stepped spillways by aeration, *J. Hydraul. Res.*, 42(3), 316–322.
- Cheng, N. S. (2006), Influence of shear stress fluctuation on bed particle mobility, *Phys. Fluids*, 18(9), doi:10.1063/1.2354434.
- Chepil, W. S. (1958), The use of evenly spaced hemispheres to evaluate aerodynamic forces on soil surfaces, *Trans. AGU*, 39(3), 397–404.
- Chiew, Y., and G. Parker (1994), Incipient sediment motion on non-horizontal slopes, *J. Hydraul. Res.*, 32(5), 649–660.
- Chiew, Y., and G. Parker (1995), Reply to “Incipient motion on non-horizontal slopes”, *J. Hydraul. Res.*, 33(5), 728–730.
- Christensen, B. A. (1995), Discussion of “Incipient motion on non-horizontal slopes”, *J. Hydraul. Res.*, 33(5), 725–728.
- Church, M., and M. A. Hassan (2002), Mobility of bed material in Harris Creek, *Water Resour. Res.*, 38(11), 1237, doi:10.1029/2001WR000753.
- Church, M., M. A. Hassan, and J. F. Wolcott (1998), Stabilizing self-organized structures in gravel-bed stream channels: Field and experimental observations, *Water Resour. Res.*, 34(11), 3169–3179.
- Cui, Y. T., and G. Parker (2005), Numerical model of sediment pulses and sediment-supply disturbances in mountain rivers, *J. Hydraul. Eng. Asce*, 131(8), 646–656.
- Cui, Y. T., G. Parker, C. Braudrick, W. E. Dietrich, and B. Cluer (2006), Dam Removal Express Assessment Models (DREAM). Part 1: Model development and validation, *J. Hydraul. Res.*, 44(3), 291–307.

- Day, T. J. (1980), A study of the transport of graded sediments, *Hydraulic Research Station Report*, Report Number IT190, p. 10, Wallingford, U.K.
- Defina, A., and A. C. Bixio (2005), Mean flow and turbulence in vegetated open channel flow, *Water Resour. Res.*, *41*(7), W07006, doi:10.1029/2004WR003475.
- Dhamotharan, S., A. Wood, G. Parker, and H. Stefan (1980), Bedload transport in a model gravel stream, *Project Report 190*, St. Anthony Falls Laboratory, Minneapolis.
- Diplas, P. (1987), Bedload transport in gravel-bed streams, *J. Hydraul. Eng.*, *113*(3), 277–292.
- Dittrich, A., and K. Koll (1997), Velocity field and resistance of flow over rough surfaces with large and small relative roughness, *Int. J. Sediment Res.*, *12*(3), 21–33.
- Drake, T. G., R. L. Shreve, W. E. Dietrich, P. J. Whiting, and L. B. Leopold (1988), Bedload transport of fine gravel observed by motion picture photography, *J. Fluid Mech.*, *192*, 193–217.
- Einstein, H. A., and N. L. Barbarossa (1952), River channel roughness, *Trans. Am. Soc. Civ. Eng.*, *117*, 1121–1146.
- Engelund, F., and J. Fredsoe (1976), A sediment transport model for straight alluvial channels, *Nord. Hydrol.*, *7*, 297–306.
- Everts, C. H. (1973), Particle overpassing on flat granular boundaries, *J. Waterw. Port Coastal Ocean Eng.*, *99*, 425–439.
- Ferguson, R. I. (1994), Critical discharge for entrainment of poorly sorted gravel, *Earth Surf. Processes Landforms*, *19*, 179–186.
- Ferguson, R. I. (2003), Emergence of abrupt gravel to sand transitions along rivers through sorting processes, *Geology*, *31*(2), 159–162.
- Fernandez Luque, R., and R. van Beek (1976), Erosion and transport of bed-load sediment, *J. Hydraul. Res.*, *14*, 127–144.
- Flammer, G. H., J. P. Tullis, and E. S. Mason (1970), Free surface, velocity gradient flow past hemisphere, *J. Hydraul. Div.*, *7*, 1485–1502.
- Furbish, D. J. (1993), Flow structure in a bouldery mountain stream with complex bed topography, *Water Resour. Res.*, *29*(7), 2249–2263.
- Furbish, D. J. (1998), Irregular bed forms in steep, rough channels — 1. Stability analysis, *Water Resour. Res.*, *34*(12), 3635–3648.
- Furbish, D. J., S. D. Thorne, T. C. Byrd, J. Warburton, J. J. Cudney, and R. W. Handel (1998), Irregular bed forms in steep, rough channels — 2. Field observations, *Water Resour. Res.*, *34*(12), 3649–3659.
- Gessler, J. (1971), Beginning and ceasing of sediment motion, in *River Mechanics*, edited by H. W. Shen, H. W. Shen, Fort Collins.
- Gilbert, G. K. (1914), The transportation of debris by running water, *U.S. Geol. Survey Prof. Pap.*, *86*, 263.
- Graf, W. L. (1979), Rapids in canyon rivers, *J. Geol.*, *87*, 533–551.
- Graf, W. H. (1991), Flow resistance over a gravel bed: Its consequences on initial sediment movement, in *Fluvial Hydraulics in Mountain Regions*, edited by A. Armanini, and G. Di Silvio, pp. 17–32, Springer-Verlag, Berlin.
- Graf, W. H., and L. Suszka (1987), Sediment transport in steep channels, *J. Hydrosoci. Hydraul. Eng.*, *5*(1), 11–26.
- Grass, A. J. (1970), Initial instability of fine sand, *J. Hydraul. Div. Am. Soc. Civ. Eng.*, *96*, 619–632.
- Hammond, F. D. C., A. D. Heathershaw, and D. N. Langhorne (1984), A comparison between shields threshold criterion and the movement of loosely packed gravel in a tidal channel, *Sedimentology*, *31*(1), 51–62.
- Hassan, M. A., and M. Church (2000), Experiments on surface structure and partial sediment transport on a gravel bed, *Water Resour. Res.*, *36*(7), 1885–1895.
- Hassan, M. A., and I. Reid (1990), The influence of microform bed roughness elements on flow and sediment transport in gravel bed rivers, *Earth Surf. Processes Landforms*, *15*(8), 739–750.
- Ho, P. Y. (1939), *Abhängigkeit der Geschiebebewegung von der Kornform und der Temperatur*, 43 pp.
- Hofland, B., J. A. Battjes, and R. Booij (2005), Measurement of fluctuating pressures on coarse bed material, *J. Hydraul. Eng. ASCE*, *131*(9), 770–781.
- Houjou, K., Y. Shimizu, and C. Ishii (1990), Calculation of boundary shear stress in open channel flow, *J. Hydrosoci. Hydraul. Eng.*, *8*(2), 21–37.
- Ikedo, S. (1982), Incipient motion of sand particles on side slopes, *J. Hydraul. Div. ASCE*, *108*(1), 95–114.
- Imaizumi, F., R. C. Sidle, S. Tsuchiya, and O. Ohsaka (2006), Hydrogeomorphic processes in a steep debris flow initiation zone, *Geophys. Res. Lett.*, *33*, L10404, doi:10.1029/2006GL026250.
- Jackson, R. G. (1976), Sedimentological and fluid-dynamic implications of turbulent bursting phenomenon in geophysical flows, *J. Fluid Mech.*, *77*(3), 531–560.
- Johnson, J. W. (1942), The importance of considering side-wall friction in bed-load investigations, *Civ. Eng.*, *12*, 329–331.
- Johnston, C. E., E. D. Andrews, and J. Pitlick (1998), In situ determination of particle friction angles of fluvial gravels, *Water Resour. Res.*, *34*(8), 2017–2030.
- Katul, G., P. L. Wiberg, J. Albertson, and G. Hornberger (2002), A mixing layer theory for flow resistance in shallow flows, *Water Resour. Res.*, *38*(11), 1250, doi:10.1029/2001WR000817.
- Kirchner, J. W., W. E. Dietrich, F. Iseya, and H. Ikeda (1990), The variability of critical shear stress, friction angle, and grain protrusion in water worked sediments, *Sedimentology*, *37*, 647–672.
- Kironoto, B. A., and W. H. Graf (1994), Turbulence characteristics in rough uniform open-channel flow, *Proc. Inst. Civ. Eng., Parts 1 and 2*, *106*(4), 333–344.
- Komar, P. D. (1979), Comparisons of the hydraulics of water flows in Martian Outflow Channels with flows of similar scale on Earth, *Icarus*, *37*(1), 156–181.
- Komar, P. D. (1987), Selective gravel entrainment and the empirical-evaluation of flow competence, *Sedimentology*, *34*(6), 1165–1176.
- Komar, P. D., and P. A. Carling (1991), Grain sorting in gravel-bed streams and the choice of particle sizes for flow-competence evaluations, *Sedimentology*, *38*(3), 489–502.
- Kondolf, G. M., and M. G. Wolman (1993), The sizes of salmonid spawning gravels, *Water Resour. Res.*, *29*(7), 2275–2285.
- Lamb, M. P., A. D. Howard, J. Johnson, K. X. Whipple, W. E. Dietrich, and J. T. Perron (2006), Can springs cut canyons into rock?, *J. Geophys. Res.*, *111*, E07002, doi:10.1029/2005JE002663.
- Lamb, M. P., A. D. Howard, W. E. Dietrich, and J. T. Perron (2007), Formation of amphitheater-headed valleys by waterfall erosion after large-scale slumping on Hawaii, *Geol. Soc. Am. Bull.*, *119*, 805–822, doi:10.1130/B25986.1.
- Lawrence, D. S. L. (2000), Hydraulic resistance in overland flow during partial and marginal surface inundation: Experimental observations and modeling, *Water Resour. Res.*, *36*(8), 2381–2393.
- Legleiter, C. J., T. L. Phelps, and E. E. Wohl (2007), Geostatistical analysis of the effects of stage and roughness on reach-scale patterns of velocity and turbulence intensity, *Geomorphology*, *83*, 322–345.
- Lenzi, M. A., L. Mao, and F. Comiti (2006), When does bedload transport begin in steep boulder-bed streams?, *Hydrol. Processes*, *20*, 3517–3533.
- Lightbody, A. F., and H. Nepf (2006), Prediction of velocity profiles and longitudinal dispersion in emergent salt marsh vegetation, *Limnol. Oceanogr.*, *21*(1), 218–228.
- Liu, T.-Y. (1935), Transportation of bottom load in an open channel, M.S. thesis, University of Iowa, Iowa City.
- Lopez, F., and M. H. Garcia (1996), Turbulence structure in cobble-bed open-channel flow, in *Civil Engineering Studies*, University of Illinois, Urbana, Illinois.
- Luque, R. F., and R. van Beek (1976), Erosion and transport of bed-load sediment, *J. Hydraul. Res.*, *14*(2), 127–144.
- Manga, M., and J. W. Kirchner (2000), Stress partitioning in streams by large woody debris, *Water Resour. Res.*, *36*(8), 2373–2379.
- Marquis, G. A., and A. G. Roy (2006), Effect of flow depth and velocity on the scales of macroturbulent structures in gravel-bed rivers, *Geophys. Res. Lett.*, *33*, L24406, doi:10.1029/2006GL028420.
- McLean, S. R., and V. Nikora (2006), Characteristics of turbulent unidirectional flow over rough beds: Double-averaging perspective with particular focus on sand dunes and gravel beds, *Water Resour. Res.*, *42*, W10409, doi:10.1029/2005WR004708.
- Meyer-Peter, E., and R. Müller (1948), Formulas for bed-load transport, *Proc. 2nd Congr. Int. Assoc. Hydraul. Res., Stockholm*, 39–64.
- Milhou, R. T. (1973), Movement of individual particles in a gravel-bottomed stream, *Trans. Am. Geophys. Union*, *54*(3), 139.
- Millar, R. G. (1999), Grain and form resistance in gravel-bed rivers, *J. Hydraul. Res.*, *37*(3), 303–312.
- Millar, R. G., and C. D. Rennie (2001), Comment on “Effects of hydraulic roughness on surface textures of gravel-bed rivers” by John M. Buffington and R. David Montgomery, *Water Resour. Res.*, *37*(5), 1527–1528.
- Miller, R. L., and R. J. Byrne (1966), The angle of repose for a single grain on a fixed rough bed, *Sedimentology*, *6*, 303–314.
- Miller, M. C., I. N. McCave, and P. D. Komar (1977), Threshold of sediment motion under unidirectional currents, *Sedimentology*, *41*, 883–903.
- Mizuyama, T. (1977), Bedload transport in steep channels, Ph.D. dissertation, Kyoto University, Kyoto, Japan.
- Mueller, E. R., and J. Pitlick (2005), Morphologically based model of bed load transport capacity in a headwater stream, *J. Geophys. Res.*, *110*, F02016, doi:10.1029/2003JF000117.
- Mueller, E. R., J. Pitlick, and J. Nelson (2005), Variation in the reference shields stress for bed load transport in gravel-bed streams and rivers, *Water Resour. Res.*, *41*, W04006, doi:10.1029/2004WR003692.
- Nakagawa, H., T. Tsujimoto, and Y. Hosokawa (1980), Statistical mechanics of bed-load transportation with 16 mm film analysis of behaviors of individual particles on a flat bed, *Third Int. Symposium on Stochastic Hydraul., Tokyo, Jpn.*, 1–12.

- Neill, C. R. (1967), Mean-velocity criterion for scour of coarse uniform bed-material, *Proc. 12th Congress Int. Assoc. Hydraul. Res.*, 3, 46–54.
- Neill, C. R. (1968), Note on initial motion of coarse uniform bed material, *J. Hydraul. Res.*, 6(2), 173–176.
- Nelson, J., W. W. Emmett, and J. D. Smith (1991), Flow and sediment transport in rough channels, in *Proceedings of the 5th interagency sedimentation conference*, pp. 55–62, Dept. of Energy.
- Nelson, J. M., R. L. Shreve, D. C. McLean, and T. G. Drake (1995), Role of near-bed turbulence structure in bed load transport and bed form mechanics, *Water Resour. Res.*, 31(8), 2071–2086.
- Nelson, J. M., M. W. Schmeeckle, and R. L. Shreve (2001), Turbulence and particle entrainment, in *Bravel-Bed Rivers V*, edited by M. P. Mosley, pp. 221–240, New Zealand Hydrological Society, Wellington, New Zealand.
- Nezu, I., and H. Nakagawa (1993), *Turbulence in Open-Channel Flows*, 281 pp., A.A. Balkema, Rotterdam.
- Nezu, I., and W. Rodi (1986), Open-channel flow measurements with a laser doppler anemometer, *J. Hydraul. Eng.*, 112(5), 335–355.
- Nikora, V., and D. Goring (2000), Flow turbulence over fixed and weakly mobile gravel beds, *J. Hydraul. Eng.*, 126(9), 679–690.
- Nikora, V., D. Goring, I. McEwan, and G. Griffiths (2001), Spatially averaged open-channel flow over rough bed, *J. Hydraul. Eng.*, 127(2), 123–133.
- Nikora, V., K. Koll, I. McEwan, S. McLean, and A. Dittich (2004), Velocity distribution in the roughness layer of rough-bed flows, *J. Hydraul. Eng.*, 130(10), 1036–1042.
- Nikuradse, J. (1933), Stromungsgesetze in rauhen Rohren, *Forsch. Arb. Ing. Wes.*, 361, 22.
- Nowell, A. R. M., and M. Church (1979), Turbulent flow in a depth-limited boundary layer, *J. Geophys. Res.*, 88(C8), 4816–4824.
- Olivero, M. L. (1984), *Movimiento Inciente de Particulas en Flujo Torrencial*, 169 pp., University of Los Andes, Merida, Venezuela.
- Paintal, A. S. (1971), Concept of critical shear stress in loose boundary open channels, *J. Hydraul. Res.*, 9, 91–113.
- Paola, C., G. Parker, R. Seal, S. K. Sinha, J. B. Southard, and P. R. Wilcock (1992), Downstream fining by selective deposition in a laboratory flume, *Science*, 258, 1757–1760.
- Papa, M., S. Egashira, and T. Itoh (2004), Critical conditions of bed sediment entrainment due to debris flow, *Nat. Hazards Earth Syst. Sci.*, 4, 469–474.
- Papanicolaou, A. N., P. Diplas, C. L. Dancy, and M. Balakrishnan (2001), Surface roughness effects in near-bed turbulence: Implications to sediment entrainment, *J. Eng. Mech. -Asce*, 127(3), 211–218.
- Papanicolaou, A. N., P. Diplas, N. Evaggelopoulos, and S. Fotopoulos (2002), Stochastic incipient motion criterion for spheres under various bed packing conditions, *J. Hydraul. Eng. -Asce*, 128(4), 369–380.
- Papanicolaou, A. N., A. B. Dour, and E. Wicklein (2004), One-dimensional hydrodynamic/sediment transport model applicable to steep mountain streams, *J. Hydraul. Res.*, 42(4), 357–375.
- Parker, G. (1978), Self-formed straight rivers with equilibrium banks and mobile bed. Part 2. The gravel river, *J. Fluid Mech.*, 89(1), 127–146.
- Parker, G. (1990), Surface-based bedload transport relation for gravel rivers, *J. Hydraul. Res.*, 28(4), 417–436.
- Parker, G., and P. C. Klingeman (1982), On why gravel bed streams are paved, *Water Resour. Res.*, 18(5), 1409–1423.
- Parker, G., and A. W. Peterson (1980), Bar resistance of gravel-bed streams, *J. Hydrol. Div. Proc. Am. Soc. Civ. Eng.*, 106, 1559–1575.
- Parker, G., P. C. Klingman, and D. G. McLean (1982), Bedload and size distribution in paved gravel-bed streams, *ASCE J. Hydraul.*, 108(4), 544–571.
- Parker, G., P. R. Wilcock, C. Paola, W. E. Dietrich, and J. Pitlick (2007), Physical basis for quasi-universal relations describing bankfull hydraulic geometry of single-thread gravel bed rivers, *J. Geophys. Res.*, 112(F4), doi:10.1029/2006JF000549.
- Perron, J. T., M. P. Lamb, C. D. Koven, I. Y. Fung, E. Yager, and M. Adamkovic (2006), Valley formation and methane precipitation rates on Titan, *J. Geophys. Res.*, 111, E11001, doi:10.1029/2005JE002602.
- Picon, G. A. (1991), Estudio Experimental de Transporte Sedimentos en Rios de Montana, M.S. thesis, Merida, Venezuela.
- Powell, D. M., I. Reid, and J. B. Laronne (2001), Evolution of bed load grain size distribution with increasing flow strength and the effect of flow duration on the caliber of bed load sediment yield in ephemeral gravel bed rivers, *Water Resour. Res.*, 37(5), 1463–1474.
- Rao, K. N., R. Narasimha, and M. A. B. Narayanan (1971), The 'bursting' phenomenon in a turbulent boundary layer, *J. Fluid Mech.*, 48(2), 339–352.
- Raupach, M. R., R. A. Antonia, and S. Rajagopalan (1991), Rough-wall turbulent boundary layers, *Appl. Mech. Rev.*, 44(1), 1–25.
- Rosgen, D. L. (1996), *Applied River Morphology*, Wildland Hydrology, Pagosa Springs, CO.
- Schlichting, H. (1979), *Boundary-Layer Theory*, McGraw-Hill.
- Schmeeckle, M. W., and J. M. Nelson (2003), Direct numerical simulation of bedload transport using a local, dynamic boundary condition, *Sedimentology*, 50, 279–301.
- Schmeeckle, M. W., J. M. Nelson, and R. L. Shreve (2007), Forces on stationary particles in near-bed turbulent flows, *J. Geophys. Res.*, 112, F02003, doi:10.1029/2006JF000536.
- Schoklitsch, A. (1962), *Handbuch des Wasserbaues*, Springer-Verlag, Vienna.
- Sechet, P., and B. Le Guennec (1999), Bursting phenomenon and incipient motion of solid particles in bed-load transport, *J. Hydraul. Res.*, 37(5), 683–696.
- Seidl, M. A., W. E. Dietrich, and J. W. Kirchner (1994), Longitudinal profile development into bedrock: An analysis of Hawaiian channels, *J. Geol.*, 102, 457–474.
- Shen, H. W., and S. Wang (1985), Incipient sediment motion and riprap design, *J. Hydraul. Eng.*, 111(3), 520–538.
- Shields, A. (1936), Anwendung der Aehnlichkeitsmechanik und der Turbulenzforschung auf die Geschiebebewegung, *Mitt. Preuss. Versuchsanst. Wasserbau Schiffbau*, 26, 26.
- Shvidchenko, A. B., and G. Pender (2000), Flume study of the effect of relative depth on the incipient motion of coarse uniform sediments, *Water Resour. Res.*, 36(2), 619–628.
- Shvidchenko, A. B., and G. Pender (2001), Macroturbulent structure of open-channel flow over gravel beds, *Water Resour. Res.*, 37(3), 709–719.
- Shvidchenko, A. B., G. Pender, and T. B. Hoey (2001), Critical shear stress for incipient motion of sand/gravel streambeds, *Water Resour. Res.*, 37(8), 2273–2283.
- Sklar, L. S., and W. E. Dietrich (2004), A mechanistic model for river incision into bedrock by saltating bed load, *Water Resour. Res.*, 40(6), W06301, doi:10.1029/2003WR002496.
- Sklar, L. S., and W. E. Dietrich (2006), The role of sediment in controlling steady-state bedrock channel slope: Implications of the saltation-abrasion incision model, *Geomorphology*, 82(1–2), 58–83.
- Smart, G. M. (2005), A novel gravel entrainment investigation, in *River, Coastal, and Estuarine Morphodynamics, IAHR Symposium*, edited by G. Parker and M. Garcia, pp. 65–69, Taylor and Francis, London.
- Smith, J. D., and S. R. McLean (1977), Spatially averaged flow over a wavy surface, *J. Geophys. Res.*, 8(12), 1735–1746.
- Solar, L., and G. Parker (2000), The curious case of mobility reversal in sediment mixtures, *J. Hydraul. Eng.*, 126(3), 185–197.
- Song, T., U. Lemmin, and W. H. Graf (1994), Uniform flow in open channels with movable gravel bed, *J. Hydraul. Res.*, 32(6), 861–876.
- Stallman, J., C. Braudrick, D. Pedersen, Y. Cui, L. Sklar, B. Dietrich, and R. Real de Asua (2004), Geomorphic effects of boulder placement on gravel capture and retention in a regulated reach of the North Umpqua River, OR, *Eos Trans. AGU*, 85(47), Fall Meet. Suppl., Abstract H53B–1245.
- Stock, J., and W. E. Dietrich (2003), Valley incision by debris flows: Evidence of a topographic signature, *Water Resour. Res.*, 39(4), 1089, doi:10.1029/2001WR001057.
- Straub, L. G., and A. G. Anderson (1958), Experiments on self-aerated flow in open channels, *J. Hydrol. Div., Proc. Am. Soc. Civ. Eng.*, 84, (HY7, paper 1890).
- Straub, L. G., and O. P. Lamb (1956), Studies of air entrainment on open-channel flows, *Am. Soc. Civ. Eng. Trans.*, 121, 30–44.
- Straub, L. G., J. M. Killen, and O. P. Lamb (1954), Velocity measurement of air-water mixtures, *Trans. Am. Soc. Civ. Eng.*, 119, 207–220.
- Sutherland, A. J. (1967), Proposed mechanism for sediment entrainment by turbulent flows, *J. Geophys. Res.*, 72, 6183–6194.
- Tachie, M. F., D. J. Bergstrom, and R. Balachandar (2000), Rough wall turbulent boundary layers in shallow open channel flow, *J. Fluids Eng.*, 122(3), 533–541.
- Tachie, M. F., D. J. Bergstrom, and R. Balachandar (2004), Roughness effects on the mixing properties in open channel turbulent boundary layers, *J. Fluids Eng.*, 126(6), 1025–1032.
- Torri, D., and J. Poesen (1988), Incipient motion conditions for single rock fragments in simulated rill flow, *Earth Surf. Processes Landforms*, 13(3), 225–237.
- Tsujiimoto, T. (1991), Bed-load transport in steep channels, in *Lecture Notes in Earth Science*, edited by S. Bhattacharji, G. M. Friedman, H. J. Neugebauer, and A. Seilacher, Springer-Verlag, Berlin.
- U.S. Waterways Experimentation Station (USWES) (1935), *Study of River-Bed Material and Their Use with Special Reference to the Lower Mississippi River*, 161 pp., Vicksburg, Miss.
- Valle, B. L., and G. B. Pasternack (2006), Air concentrations of submerged and unsubmerged hydraulic jumps in a bedrock step-pool channel, *J. Geophys. Res. -Earth Surf.*, 111(F3).

- Vanoni, V. A., and N. H. Brooks (1957), Laboratory studies of the roughness and suspended load of alluvial streams, in *Calif. Inst. Technology Sedimentation Laboratory, Report E-68*, p. 121 (also US Army Corps of Eng., M.R.D. Sediment Series 11, 121 pp.), California Institute of Technology, Pasadena, California.
- Vollmer, S., and M. Kleinhans (2007), Predicting incipient motion, including the effect of turbulent pressure fluctuations in the bed, *Water Resour. Res.*, *43*, W05410, doi:10.1029/2006WR004919.
- Wang, J. J., and Z. N. Dong (1996), Open-channel turbulent flow over non-uniform gravel beds, *Appl. Sci. Res.*, *56*(4), 243–254.
- Wang, J., C. K. Chen, Z. N. Dong, and X. Zhenhuan (1993), The effects of bed roughness on the distribution of turbulent intensities in open-channel flow, *J. Hydraul. Res.*, *31*(1), 89–98.
- Wathen, S. J., R. I. Ferguson, T. B. Hoey, and A. Werritty (1995), Unequal mobility of gravel and sand in weakly bimodal river sediments, *Water Resour. Res.*, *31*(8), 2087–2096.
- Wiberg, P. L., and J. D. Smith (1987a), Calculations of the critical shear stress for motion of uniform and heterogeneous sediments, *Water Resour. Res.*, *23*, 1471–1480.
- Wiberg, P. L., and J. D. Smith (1987b), Initial motion of coarse sediment in streams of high gradient, *Erosion and Sedimentation in the Pacific Rim (Proceedings of the Corvallis Symposium) IAHS Publication Number, 165*, 299–308.
- Wiberg, P. L., and J. D. Smith (1991), Velocity distribution and bed roughness in high gradient streams, *Water Resour. Res.*, *27*, 825–838.
- Wiele, S. M., P. R. Wilcock, and P. E. Grams (2007), Reach-averaged sediment routing model of a canyon river, *Water Resour. Res.*, *43*(2), W02425, doi:10.1029/2005WR004824.
- Wilcock, P. R. (1987), Bed-load transport in mixed-size sediment, Ph.D. thesis, MIT, Cambridge.
- Wilcock, P. R. (1993), Critical shear-stress of natural sediments, *J. Hydraul. Eng.*, *119*(4), 491–505.
- Wilcock, P. R. (1998), Two-fraction model of initial sediment motion in gravel-bed rivers, *Science*, *280*(5362), 410–412.
- Wilcock, P. R. (2001), Comment on “Effects of hydraulic roughness on surface textures of gravel-bed rivers” and “Effects of sediment supply on surface textures of gravel-bed rivers” by John M. Buffington and R. David Montgomery, *Water Resour. Res.*, *37*(5), 1525–1526.
- Wilcock, P. R., and J. C. Crowe (2003), Surface-based transport model for mixed-size sediment, *J. Hydraul. Eng.*, *129*(2), 120–128.
- Wilcock, P. R., and B. W. McArdeall (1993), Surface-based fractional transport rates - Mobilization thresholds and partial transport of a sand-gravel sediment, *Water Resour. Res.*, *29*(4), 1297–1312.
- Wilcock, P. R., and J. B. Southard (1988), Experimental-study of incipient motion in mixed-size sediment, *Water Resour. Res.*, *24*(7), 1137–1151.
- Wilcock, P. R., S. T. Kenworthy, and J. C. Crowe (2001), Experimental study of the transport of mixed sand and gravel, *Water Resour. Res.*, *37*(12), 3349–3358.
- Wilcox, A. C., J. M. Nelson, and E. E. Wohl (2006), Flow resistance dynamics in step-pool channels: 2. Partitioning between grain, spill, and woody debris resistance, *Water Resour. Res.*, *42*(5), W05419, doi:10.1029/2005WR004278.
- Wittler, R. J., and S. R. Abt (1995), Shields parameter in low submergence or steep flows, in *River, Coastal and Shoreline Protection: Erosion Control Using Riprap and Armourstone*, edited by C. R. Thorne, S. R. Abt, S. T. Barends, S. T. Maynard, and K. W. Pilarczyk, pp. 93–101, John Wiley & Sons, New York.
- Wohl, E. E., and D. M. Thompson (2000), Velocity characteristics along a small step-pool channel, *Earth Surf. Processes Landforms*, *25*(4), 353–367.
- Wu, F. C., and K. H. Yang (2004), Entrainment probabilities of mixed-size sediment incorporating near-bed coherent flow structures, *J. Hydraul. Eng. -Asce*, *130*(12), 1187–1197.
- Yager, E. M., J. W. Kirchner, and W. E. Dietrich (2007), Calculating bed load transport in steep boulder bed channels, *Water Resour. Res.*, *43*(7), W07418, doi:10.1029/2006WR005432.
- Yalin, M. S. (1977), *Mechanics of Sediment Transport*, 298 pp., Pergamon Press, Oxford.
- Yalin, M. S., and E. Karahan (1979), Inception of sediment transport, *J. Hydraul. Div. -ASCE*, *105*(11), 1433–1443.
- Zanke, U. C. E. (2003), On the influence of turbulence on the initiation of sediment motion, *Int. J. Sediment Res.*, *18*(1), 17–31.
- Zimmermann, A., and M. Church (2001), Channel morphology, gradient profiles and bed stresses during flood in a step-pool channel, *Geomorphology*, *40*(3–4), 311–327.

W. E. Dietrich and M. P. Lamb, Earth and Planetary Science, University of California, 307 McCone Hall, Berkeley, CA 94720-4767, USA. (mpl@berkeley.edu)

J. G. Venditti, Department of Geography, Simon Fraser University, Burnaby, BC, Canada.